for l_d and III_c are given in Tables IV and V, respectively.

Acknowledgment. K.-W.L. acknowledges Professor John R. Shapley for helpful discussions. High-field NMR facilities were provided by the National Science Foundation (NSF Grant CHE 79-16100). High-resolution mass spectrometer facilities were supported in part by a grant from the National Institute of General Medicine Sciences (GM 27029). The ZAB-HF mass spectrometer was purchased in part with grants from the Division of Resources, National Institutes of Health (RR 01575), and the National Science Foundation (PCM 8121494).

Registry No. Ia, 94090-56-9; Ib, 94090-57-0; Ib', 94160-63-1; Ic, 94090-58-1; Id, 94090-59-2; IIa, 94090-60-5; IIb, 94111-25-8; IIc, 94136-21-7; IId, 94111-26-9; IIIa, 94136-23-9; IIIb, 94136-24-0; IIIc, 94136-25-1; IVa, 94111-27-0; IVb, 94111-28-1; IVc, 94136-22-8; IVd, 94111-29-2; V, 94111-30-5; VIa, 94136-27-3; VIb, 94136-26-2; $Re_2(CO)_7(\mu\text{-dppm})(PMe_3)$, 94111-31-6; $Re_2(CO)_7(\mu\text{-dppm})(PPh_3)$, 94111-32-7; $Re_2(CO)_7(\mu\text{-dppm})(HPPh_2)$, 94136-28-4; $Cl(OC)_4RePPh_2CH_2Ph_2PRe(CO)_4Cl$, 94111-33-8; $Re_2(CO)_6(\mu\text{-dppm})(\mu\text{-Cl})_2$, 94111-34-9; $Re_2(CO)_8(\mu\text{-dppm})$, 82292-83-9; $Re_2(CO)_8(\mu\text{-dmpm})$, 88271-76-5; PPh_3, 603-35-0; PMe_3, 594-09-2; $HPPh_2$, 829-85-6; CCl_4, 56-23-5; acetylene, 74-86-2; phenylacetylene, 536-74-3.

Supplementary Material Available: Table A, atomic positional parameters for I_d; Table B, anisotropic thermal parameters for I_d; Table C, calculated hydrogen atom positions for I_d; Table D, atomic positional parameters for III_c; Table E, anisotropic thermal parameters for III_c; Table F, calculated hydrogen atom positions for III_c (12 pages). Ordering information is given on any current masthead page.

Supported Organoactinides. Surface Chemistry and Catalytic Properties of Alumina-Bound (Cyclopentadienyl)- and (Pentamethylcyclopentadienyl)thorium and -uranium Hydrocarbyls and Hydrides

Ming-Yuan He,[1a] Guoxing Xiong,[1b] Paul J. Toscano, Robert L. Burwell, Jr.,* and Tobin J. Marks*

Contribution from the Department of Chemistry, Northwestern University, Evanston, Illinois 60201. *Received July 10, 1984*

Abstract: This contribution reports a detailed, quantitative investigation of surface chemistry and catalysis involving selected organoactinides and partially dehydroxylated (PDA) or dehydroxylated (DA) alumina supports. For the complexes $Cp'_2M(CH_3)_2$ and $Cp'_2M(CD_3)_2$ ($Cp' = \eta^5\text{-}(CH_3)_5C_5$; M = Th, U), methane-evolving surface reaction pathways are identified as M–CH_3 protonolysis via surface OH (especially on PDA), Cp' H atom abstraction, and intramolecular elimination of methane within $M(CH_3)_2$ units. This latter process is proposed on the basis of methylene transfer to acetone and some olefin metathesis activity to result in Al^{3+}-stabilized alkylidenes. Hydrogenolysis studies indicate that ca. 25% of the $Cp'_2M(CH_3)_2$/DA surface M–CH_3 groups are removable as methane; reduction of methyl chloride to methane confirms the presence of surface M–H groups produced by hydrogenolysis. The $Cp'_2M(CH_3)_2$/DA complexes are active catalysts for propylene hydrogenation following a variety of pretreatment conditions, with $N_t \approx 0.5\ s^{-1}$ in a flow reactor at −63 °C (about 10 times more active than typical Pt/SiO_2 catalysts under the same conditions). M = Th and U are comparable in hydrogenation activity, and CO poisoning experiments indicate that ca. 3% of the adsorbed molecules is catalytically active. $Cp'_2M(CH_3)_2$ complexes on PDA and silica gel are considerably less active catalysts. The $Cp'_2M(CH_3)_2$/DA systems are also active catalysts for ethylene polymerization and weakly active for butene isomerization. Experiments with $Cp'_2Th[CH_2C(CH_3)_3]_2$ and $[Cp'_2Th(\mu\text{-}H)H]_2$ on DA reveal activity for propylene hydrogenation comparable to the $Cp'_2M(CH_3)_2$ systems. In contrast, more coordinatively saturated Cp_3UCH_3 and $Cp_3Th(n\text{-}C_4H_9)$ ($Cp = \eta^5\text{-}C_5H_5$) are far less active, while $Cp'Th(CH_2C_6H_5)_3$ is far more active ($N_t \approx 10\ s^{-1}$). Much of the stoichiometric and catalytic surface chemistry can be understood in terms of solution organoactinide reactivity patterns.

There is currently great interest in the structural, chemical, and catalytic properties of the unusual species formed when carbonyl and non-carbonyl transition-metal organometallic compounds are adsorbed on the surfaces of porous metal oxides such as γ-alumina, silica, magnesia, zeolites, etc.[2] In a number of cases, these supported species exhibit dramatic reactivity enhancements over the precursor molecules in homogeneous solution, and high catalytic activity for such processes as the hydrogenation, metathesis, isomerization, and polymerization of olefins is observed. Several of these organometallic/metal oxide systems are also of technological significance.[2,3] The accurate characterization of such highly reactive molecule/support complexes has presented a great challenge and, in all but a few cases, the present structural/mechanistic picture remains highly speculative.

In homogeneous solution, organoactinides display a rich variety of unusual stoichiometric and catalytic reactivity patterns.[4]

(1) (a) Visiting scholar on leave from the Research Institute of Petroleum Processing, Beijing, PRC. (b) Visiting scholar on leave from the Institute of Chemical Physics, Dalian PRC.

(2) (a) Yermakov, Yu. I. *J. Mol. Catal.* **1983**, *21*, 35–55 and references therein. (b) Basset, J. M.; Chaplin, A. *J. Mol. Catal.* **1983**, *21*, 95–108 and references therein. (c) Iwamoto, M.; Kusano, H.; Kagawa, S. *Inorg. Chem.* **1983**, *22*, 3365–3366 and references therein. (d) Yermakov, Yu. I.; Kuznetsov, B. N.; Zakharov, V. A. "Catalysis by Supported Complexes"; Elsevier: Amsterdam, 1981. (e) Bailey, D. C.; Langer, S. H. *Chem. Rev.* **1981**, *81*, 109–148. (f) Zakharov, V. A.; Yermakov, Yu. I. *Catal. Rev.—Sci. Eng.* **1979**, *19*, 67–103. (g) Hartley, F. R.; Vezry, P. N. *Adv. Organomet. Chem.* **1978**, *15*, 189–234. (h) Ballard, D. G. H. *J. Polym. Sci., Polym. Chem. Ed.* **1975**, *13*, 2191–2212. (i) Ballard, D. G. H. *Adv. Catal.* **1973**, *23*, 263–325.

(3) (a) Gavens, P. D.; Bottrill, M.; Kelland, J. W.; McMeeking, J. In "Comprehensive Organometallic Chemistry"; Wilkinson, G., Stone, F. G. A., Abel, E. W., Eds.; Pergamon Press: Oxford, 1982; Chapter 22.5. (b) Galli, P.; Luciani, L.; Cecchini, G. *Angew. Makromol. Chem.* **1981**, *94*, 63–89. (c) Karol, F. J.; Wu, C.; Reichle, W. T.; Maraschin, N. J. *J. Catal.* **1979**, *60*, 68–76. (d) Boor, J., Jr. "Ziegler-Natta Catalysts and Polymerizations"; Academic Press: New York, 1979; Chapters 6, 22. (e) Firment, L. E. *J. Catal.* **1983**, *82*, 196–212 and references therein.

0002-7863/85/1507-0641$01.50/0

Regarding the question of whether organoactinides might display interesting surface chemical properties, we recently reported that bis(pentamethylcyclopentadienyl)thorium and -uranium alkyls, when supported upon γ-alumina, display high catalytic activity for olefin hydrogenation and polymerization.[5] The nature of these adsorbed species is of interest not only within the context of the new 5f surface chemistry currently evolving but also because certain distinctive chemical and spectroscopic characteristics of actinide ions may afford a better understanding, in general, of how metal oxide surfaces modify the properties of organometallic molecules. In the present contribution, we present a descriptive and mechanistic account of chemistry and catalysis using a series of organoactinides selected for varying metal redox characteristics, coordinative unsaturation, and two-electron ligands, adsorbed upon alumina surfaces offering varying ligation environments. Several experiments are also reported for silica gel. A preliminary account of surface chemistry involving two actinide methyl compounds and alumina has been recently reported.[6] In an accompanying contribution,[7] we report a complementary high-resolution solid-state ^{13}C NMR study of some of the organoactinide/alumina surface complexes described herein. This provides important complementary information on the surface chemistry.

Experimental Section

Surface Chemical and Catalytic Techniques. The flow apparatus and procedures employed were generally similar to those previously described.[8] Experiments could be run either in the pulse or in the flow mode. In the pulse mode, the pressure of a gas in the loop of the injection valve (Carle Microvolume, purged with helium) could be adjusted and then read with a capacitance manometer. This permitted a wide variation in pulse size, from 1 to 40 μmol. This pulse was injected into flowing hydrogen or helium. The hydrogenation of propylene could be run in the flow mode by passing hydrogen through a bed of porous Filtros thermostated at −78 °C and saturated with liquid propylene.[9] The ratio, H_2/C_3H_6, was 4.6. Valves were Kontes Teflon-brand valves, Nupro bellows valves, or Whitey three-way ball valves. The apparatus was constructed mostly of $^1/_4$-in. Pyrex tubing joined by Swagelock fittings with Teflon-brand ferrules.

For catalytic reactions, we typically employed 10–20 μmol of actinide complex on 0.25 g of 60–80 mesh American Cyanamid PHF γ-alumina, 99.99% pure, which had been treated as previously described.[8] In surface chemistry experiments we usually employed 25–50 μmol of organoactinide/0.25 g of alumina. Partially dehydroxylated alumina (PDA) and dehydroxylated alumina (DA) were prepared by heating to predetermined temperatures in flowing helium (vide infra). These supports were deuterated by the literature procedure.[10] Flow rates of carrier in pulse experiments or of propylene plus hydrogen in flow hydrogenations were usually 0.1–0.4 mol h^{-1}. The actinide complexes employed in this study are exceedingly oxygen sensitive. Therefore, the presence of O_2 at a parts per million level could cause serious deactivation in experiments lasting 1 day. Oxygen in gases that flow continuously over the catalyst is much more serious than O_2 in gases used only as pulses. The final means of reducing the content of O_2 was a trap of 10% MnO/SiO_2 which reduces the content of O_2 to the parts per billion range and which just preceded the catalytic reactor.[11]

Reactants and Carrier Gas. The organoactinide complexes $Cp'_2Th(CH_3)_2$[12] ($Cp' = \eta^5$-$(CH_3)_5C_5$), $Cp'_2U(CH_3)_2$,[12] $Cp'_2Th[CH_2C(CH_3)_3]_2$,[12] $Cp'_2U(CH_3)Cl$,[12] $[Cp'_2Th(\mu\text{-}H)H]_2$,[12] $Cp'Th(CH_2C_6H_5)_3$,[13] $Cp_3Th(n\text{-}C_4H_9)$[14] ($Cp = \eta^5$-C_5H_5), and Cp_3UCH_3[15] were prepared and purified by the literature procedures. Complexes incorporating the CD_3 functionality were prepared with CD_3Li (from CD_3I (Cambridge Isotope Laboratories) and Li in diethyl ether[16]). These materials were handled in Schlenk ware interfaced to a high-vacuum line or in a Vacuum Atmosphere inert atmosphere box equipped with a high-capacity atmosphere recirculator.

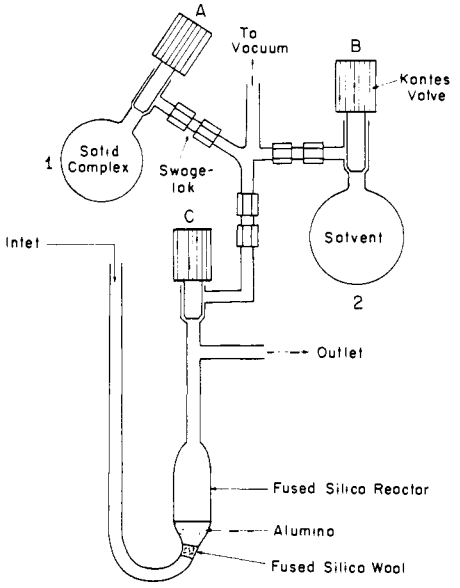

Figure 1. Diagram of flow reactor used in catalytic studies. Letter and number labels are identified under Catalyst Preparation and Activation in the Experimental Section.

Acetone was distilled anaerobically from 4A molecular sieves into and stored in a flask provided with a Kontes Teflon valve. Pentane was sequentially treated with concentrated H_2SO_4, $KMnO_4$ solution, $MgSO_4$, and Na + molecular sieves. It was then saturated with N_2 and, under inert gas flush, poured into a flask containing P_2O_5 and stirred overnight. It was finally subjected to three freeze–pump–thaw cycles and vacuum transferred to a flask containing Na/K alloy. After stirring overnight, the pentane was considered ready for catalytic experiments. It was vacuum transferred to flask 2 of the reaction apparatus (Figure 1) and stored over Cp'_2UCl_2 as an indicator. GC analysis revealed only minute traces of pentene as a contaminant. The purity of the pentane was found to be critical. Benzene was purified by multiple vacuum distillations from Na/K alloy.

In pulse experiments, propylene was purified only by a MnO/SiO_2 trap just preceding the catalyst bed. In flow hydrogenation, which involved exposure of the catalyst to much larger amounts of propylene, the propylene was first purified in the apparatus by freeze–thaw operations to remove one-fourth of the propylene originally condensed. Following this, propylene was condensed in the Filtros bed during which the residual one-fifth of the propylene was discarded. Before directing the $H_2 + C_3H_6$ flow to the catalyst, hydrogen was passed through the Filtros saturator at −78 °C for 30 min and vented to remove any lower boiling gases.

Helium was initially purified by passage through a trap of Davison grade 62 silica gel (average pore diameter, 14 nm) at −196 °C followed by a MnO/SiO_2 trap. Another MnO/SiO_2 trap just preceded the pulse injection valve.

Hydrogen was supplied by an Elhygen (Milton Roy) electrolytic generator in which the hydrogen passed through Pd,Ag alloy. In the pulse mode, hydrogen was passed through an MnO/SiO_2 trap just before the injection valve or, in the flow mode, just before the saturator.

(4) (a) Marks, T. J.; Ernst, R. D. in "Comprehensive Organometallic Chemistry"; Wilkinson, G., Stone, F. G. A., Abel, E. W., Eds.; Pergamon Press: Oxford, 1982; Chapter 21. (b) Marks, T. J. *Science (Washington, D.C.)* **1982**, *217*, 989–997. (c) Marks, T. J., Fischer, R. D., Eds. "Organometallics of the f-Elements": Reidel: Dordrecht, 1979. (d) Marks, T. J. *Prog. Inorg. Chem.* **1979**, *25*, 224–333.

(5) (a) Bowman, R. G.; Nakamura, R.; Fagan, P. J.; Burwell, R. L., Jr.; Marks, T. J. *J. Chem. Soc., Chem. Commun.* **1981**, 257–258. (b) Bowman, R. G.; Fagan, P. J.; He, M.-Y.; Nakamura, R.; Stecher, H. A.; Burwell, R. L., Jr.; Marks, T. J. *Abstr. Pap.—Am. Chem. Soc.* **1981**, *182nd*, INOR 4.

(6) He, M.-Y.; Burwell, R. L., Jr.; Marks, T. J. *Organometallics* **1983**, *2*, 566–569.

(7) Toscano, P. J.; Marks, T. J., accompanying article.

(8) Bowman, R. G.; Burwell, R. L., Jr. *J. Catal.* **1980**, *63*, 463–475.

(9) Patterson, W. R.; Roth, J. A.; Burwell, R. L., Jr. *J. Am. Chem. Soc.* **1971**, *93*, 839–846.

(10) (a) Laniecki, M.; Burwell, R. L., Jr. *J. Colloid Interface Sci.* **1980**, *75*, 95–104. (b) Hall, W. K.; Leftin, H. P.; Cheselske, F. J.; O'Reilly, D. E. *J. Catal.* **1963**, *2*, 506–517.

(11) Moeseler, R.; Horvath, B.; Lindenau, D.; Horvath, E. G.; Krauss, H. L. *Z. Naturforsch., B* **1976**, *31B*, 892–893.

(12) Fagan, P. J.; Manriquez, J. M.; Maatta, E. A.; Seyam, A. M.; Marks, T. J. *J. Am. Chem. Soc.* **1981**, *103*, 6650–6667.

(13) (a) Mintz, E. A.; Moloy, K. G.; Marks, T. J.; Day, V. W. *J. Am. Chem. Soc.* **1982**, *104*, 4692–4695. (b) Sternal, R. S.; Marks, T. J., manuscript in preparation.

(14) Marks, T. J.; Wachter, W. A. *J. Am. Chem. Soc.* **1976**, *98*, 703–710.

(15) Marks, T. J.; Seyam, A. M.; Kolb, J. R. *J. Am. Chem. Soc.* **1973**, *95*, 5529–5539.

(16) The CD_3 ligands in $Cp'_2Th(CD_3)_2$ and $Cp'_2U(CD_3)_2$ were found to be >98% trideuterated by ^1H NMR (integrating metal–methyl vs. ring–methyl resonances) or by GC/MS analysis of evolved CD_3H (following hydrolysis).

Carbon monoxide, ethylene, butylene, and methyl chloride were used only in the pulse mode. Any oxygen or water in these gases would be removed by the final MnO/SiO_2 trap. Deuterium was also purified only by the MnO/SiO_2 trap just preceding the reactor.

Measurement of the Oxygen Content of Carrier Gases. The oxygen content at any position in the system could be measured by inserting a 0.6% MnO/SiO_2 trap, passing hydrogen or helium at a known flow rate through the trap, and measuring the rate of advancement of a brown band. The process was calibrated by injection of a known, small pulse of O_2. MnO/SiO_2 is brown in the oxidized form, green in the reduced form. Content in oxygen at the entrance to the reactor was less than 0.03 ppm.

Catalyst Preparation and Activation. These operations were effected in the apparatus of Figure 1 which was connected to the rest of the apparatus at the inlet and outlet by means of flexible $^1/_{16}$-in. stainless steel tubing and Swagelock unions. Alumina (0.25 g) was placed in the reactor, a flow of helium was established through it and it was activated with He,475°,1 (flowing helium 475 °C, 1 h) to give PDA (partially dehydroxylated alumina) or with He, ~1000°,0.3 to give DA (dehydroxylated alumina).[8,10a,17] Dehydroxylation at 950 and 1025 °C appeared to give the same results within experimental reproducibility. These activation codes give the flowing gas, the temperature (°C), and the duration of activation in hours. Bulb 1 and the plunger of valve A were transferred to the glovebox along with a vial provided with an air-tight cap. About 10–30 mg of complex was added to the vial, which was then capped, removed from the glovebox, and accurately weighed. The vial was then returned to the glovebox and opened and the complex was transferred to bulb 1, a magnetic stirring bar was added, the plunger was inserted and rotated to the closed position. The amount of complex added was found by removing the vial from the glovebox and weighing it. Bulb 1 was then reattached to the position shown in Figure 1. Valves A, B, and C were closed and the region between them was evacuated overnight. Helium was admitted and then evacuated to 5×10^{-4} torr. Valve A was opened and evacuation–filling with helium was repeated 3 times. After a final evacuation, pentane (usually 5–6 cm^3) was distilled from bulb 2 to bulb 1 by cooling bulb 1 to 78 K. After warming, the complex was dissolved in the pentane by use of the stirring bar. A flow of helium was then initiated through the reactor with valve C open. Bulb 1 was rotated up so as to deliver its contents to the reactor, which was maintained at 0 °C, and the flow of helium was increased so as to fluidize the alumina. The purpose of fluidization was to make the distribution of complex on the alumina as uniform as possible. The complex was fully adsorbed within a few seconds. The flow of helium was reduced to about 30 cm^3 min^{-1} and continued until the alumina appeared dry. The resulting complex/alumina was then activated in flowing helium or hydrogen.

During catalyst preparation and activation, the effluent from the reactor passed through an empty trap at −196 °C to remove pentane and then a −196 °C silica gel trap to remove methane and other hydrocarbons. Warming released these as a pulse which could be analyzed catharometrically either directly or after passage through a gas chromatographic column. Pulses containing CH_4, CO, N_2, and O_2 were separated on a 2-ft column of molecular sieve 13X. When it was desired to analyze for hydrogen in the helium carrier, the effluent stream from the silica gel trap was passed through molecular sieve 5A at 78 K. Warming released a pulse of hydrogen which was converted to one of water by CuO at 500 °C before the thermal conductivity cell. A 4-ft column of bis[(2-methoxyethoxy)ethyl] ether on 60–80 mesh Gas-Chrom R. A. (Applied Science Laboratories) was used to separate hydrocarbons. Where GC/MS analysis was to be performed, hydrocarbons were removed by a silica gel trap at 78 K which could be isolated and detached for transferral to the GC/MS unit.

Hydrogenation and Polymerization. In flow hydrogenation, effluent from the reactor passed through the loop of an injection valve which permitted samples to be injected into a stream of helium passing through the aforementioned chromatographic column so as to analyze the propane and propylene. During flow hydrogenations, the reactor was usually maintained at −63 °C either with a chloroform slush bath or by means of a CryoCool refrigerator with a CryoCool temperature controller.

In studies of the polymerization of ethylene, a series of about 20 pulses of ethylene were injected into helium flowing over the catalyst at 30 cm^3 min^{-1}. Unadsorbed ethylene was then separated on a silica gel GC column. The amount of ethylene in each exit pulse was determined, and the loss of ethylene was calculated. In some cases, the ethylene passing through the catalyst in a series of pulses was collected in a silica trap at −196 °C and then released as a pulse for catharometric analysis by warming the trap. The moles of ethylene in a pulse was adjusted to be about equal to the moles of the actinide element on the catalyst. The total C_2H_4/M ratio (M = U or Th) was then calculated.

Adsorption of Carbon Monoxide. The amount of carbon monoxide adsorbed on a catalyst was determined by a pulse technique either in helium or in hydrogen carrier. The pulse size was adjusted so that most of the first pulse was adsorbed and retained by the catalyst. The amount of a pulse that passed unadsorbed through the catalyst bed was measured catharometrically. Several further pulses were injected until no further adsorption was evident. The temperature of the catalyst was usually 25 °C during these experiments.

Spectrophotometric Studies of Cp′H Ring Loss. A special, anaerobic "H-shaped" optical spectroscopy cell was constructed with Kontes valve high-vacuum connections. One leg of the "H" consisted of a vacuum-tight fused-silica cuvette (sealed on) and the other a Pyrex reaction chamber. This allowed reagents to be distilled in or products removed on the high-vacuum line. Spectra could be recorded by pouring supernatant solutions into the cuvette leg. In a typical experiment, the optical cell was charged with a weighed amount of $Cp'_2Th(CH_3)_2$ (typically ~40–50 μmol) and DA or PDA (0.5 g) in the glovebox. It was then attached to the high-vacuum line and evacuated and a known amount of pentane transferred by trap-to-trap distillation at 77 K. The apparatus was then back-filled with Ar, removed from the line, and shaken by hand for ~1 h. At this time, a UV spectrum from 350 to 220 nm was obtained (in general, spectra did not change over the subsequent 12 h).

To calculate the yield of Cp′H released on adsorbing $Cp'_2Th(CH_3)_2$ on DA or PDA, the following procedure was carried out. Using the data system of the spectrophotometer, the UV spectrum of a pure sample of Cp′H in pentane (at known concentration) was recorded. Next, spectra of pentane and pentane + DA were recorded. These latter spectra were essentially identical except for a very weak absorption in the pentane due to pentene, which disappeared upon treatment with DA. The change in absorbance (A) was, however, very small—1–2%. Next, spectra of $Cp'_2Th(CH_3)_2$/DA or $Cp'_2Th(CH_3)_2$/PDA supernatants were recorded, and the pentane spectrum was subtracted from them. The concentration and yield of Cp′H was then calculated using A values at several points in the spectrum and taking the average. For $Cp'_2Th(CH_3)_2$/DA, this procedure gave the following percentages of Cp′H released for four different experiments: 0.16%, 0.25%, <0.1%, <0.1%. For $Cp'_2Th(CH_3)_2$/PDA, two experiments yielded 2.6% and 2.0% cleavage. Reference to control spectra of $Cp'_2Th(CH_3)_2$ in pentane revealed that negligible quantities of the organoactinide remained unadsorbed.

The foregoing analysis makes the assumption that free Cp′H is not adsorbed by the $Cp'_2M(CH_3)_2$–covered alumina under the reaction conditions. In a separate experiment, it was found that after 1 h of shaking, ca. 80% of a 9-μmol sample of Cp′H in pentane was adsorbed by 0.5 g of pure DA. However, under the same conditions, negligible Cp′H adsorption was measured for DA samples pretreated with $Cp'_2Th(CH_3)_2$ at the usual loading.

Instrumental Measurements. The purity and/or isotopic composition (e.g., $Cp'_2M(CD_3)_2$) of all organoactinides was routinely monitored by ^1H NMR using a JEOL FX-90 or FX-270 spectrometer. Solutions were studied in benzene-d_6. Spectrophotometric experiments were carried out with a Perkin-Elmer Hitachi Model 330 UV–vis–near-IR spectrophotometer and interfaced Perkin-Elmer data system.

Mass spectrometric studies were conducted with a Hewlett-Packard Model 5985 gas chromatograph/mass spectrometer and interfaced data system. Deuterium incorporation studies employed a nominal ionizing voltage of 12 eV and procedures discussed previously.[18] For methane analyses, authentic samples of CD_4, CD_3H, and CH_3D were employed as reference compounds. In making corrections for fragment ions of isotopically exchanged species, it was assumed that the probability of C–D fragmentation was 0.85 that of C–H. Methane samples were injected directly into the mass spectrometer. Interference from water (m/e 18 amu) considerably limited the accuracy of CH_2D_2 assays.

Results

We begin this section with a brief synopsis of the chemical properties of organoactinide complexes and of alumina which are crucial to the design and analysis of the present experiments. We then focus upon organoactinide + alumina surface reaction pathways, using $Cp'_2M(CH_3)_2$ compounds as models. The properties of the adsorbed species are next probed using several diagnostic stoichiometric reagents. Finally, the catalytic properties of a selected group of alumina-supported organoactinides are examined, using propylene hydrogenation, butene isomerization, and ethylene polymerization as prototype transformations.

(17) Peri, J. B.; Hannan, R. B. *J. Phys. Chem.* **1960**, *64*, 1526–1530.

(18) (a) Burwell, R. L., Jr.; Briggs, W. S. *J. Am. Chem. Soc.* **1952**, *74*, 5096–5102. (b) Bruno, J. W.; Kalina, D. G.; Marks, T. J. *J. Am. Chem. Soc.* **1982**, *104*, 1860–1869.

Organoactinides and Supports. Three basic classes of organoactinides were chosen for this study (A–C). Of these, the

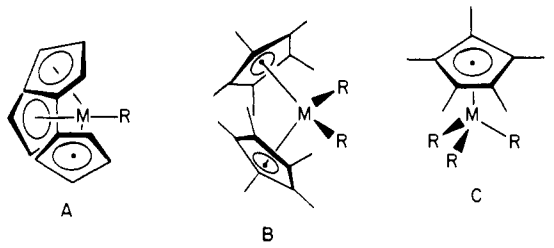

tris(cyclopentadienyls) (Cp_3MR, A)[14,15] and the bis(pentamethylcyclopentadienyls) (Cp'_2MR_2, B)[12] have been best characterized in terms of reactivity, reaction kinetics, and mechanism, as well as disruption enthalpies of metal–ligand bonds.[19] In several typical reaction patterns (eq 1 and 2), dramatic rate enhancements,

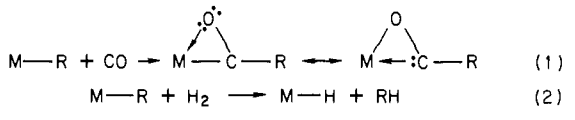

(1)

(2)

presumably reflecting differences in coordinative unsaturation, are observed for system B over A. Indeed migratory CO insertion[4,20] is typically $\gtrsim 10^4$ more rapid for B,[21] and metal–carbon bond hydrogenolysis, while rapid for B,[12] has never been observed for A.[18b] Also noteworthy is the observation that π-donating alkoxide ligands effect a marked decrease (ca. 10^6) in the rate of eq 2 for system B (viz., $Cp'_2M(OR')R \rightarrow Cp'_2M(OR')H$).[12] Hydrides derived from system B undergo rapid CO[21b,22,23] and olefin insertion[12] (eq 3 and 4). Equation 3 is ca. 10^8 times more

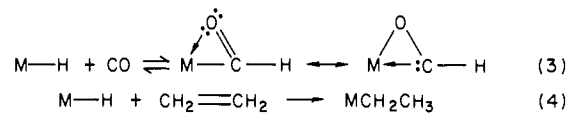

(3)

(4)

rapid for M–H than M–CH_3 bonds in the same coordination environment.[21b] For $[Cp'_2M(\mu\text{-}H)H]_2$, eq 4 and 2 can be coupled to effect homogeneous olefin hydrogenation with $N_t = 1.5 \times 10^{-4}$ s^{-1} (M = Th) for 1-hexene in toluene at 1 atm of H_2, 24 °C.[12] Although Cp'_2MR_2 compounds are essentially inactive for ethylene polymerization,[12] trivalent $(Cp'_2UH)_n$ complexes are highly active.[24] Another characteristic reaction of organoactinide hydrides is the rapid, essentially quantitative substitution of halogen for hydride by halocarbons (eq 5).[12]

$$M\text{-}H + RX \rightarrow M\text{-}X + RH \qquad X = Cl, Br, I \qquad (5)$$

All actinide hydrocarbyls and hydrides undergo protonolysis with alcohols to yield alkoxides (e.g., eq 6).[12-15,19] Rates are

$$M\text{-}R + R'OH \rightarrow MOR' + RH \qquad R = H, \text{hydrocarbyl functionality} \qquad (6)$$

usually somewhat greater for M = Th than for U, multiple alkyl ligands are usually cleaved sequentially, and attack on Cp–M and Cp′–M linkages is far slower. Other differences between Th and U in the organometallic chemistry are generally small, with no evidence for involvement of U(V) and U(VI), but several examples are known where H_2 reductive elimination (presumably binuclear) leads to U(III) compounds.[12,25] Far less is known about $Cp'MR_3$ chemistry; however, preliminary observations[13] suggest reactivity at least as great as for Cp'_2MR_2 complexes.

Table I. Methane Yields during Activation of 16.6 μmol of $Cp'_2Th(CD_3)_2$/0.25 g of DA

step	treatment	methane/Th[a]
1	He,0°,1[b]	0.078
2	He,100°,1	0.054
3	He,100°,1	0.013
4	He,100°,2	0.014
5	He,100°,3	0.012 (0.17[c])
6	H_2,100°,1	0.169[d]

[a] Molar ratio of methane/complex during each step. [b] During the evaporation of pentane. [c] Cumulative methane/complex yield during steps 1–5. [d] Almost entirely CHD_3.

The alumina support employed in the present study is γ-alumina (cubic),[26] the surface hydroxyl coverage of which has been depleted by heating under flowing helium at 475 °C or ~1000 °C.[8,10a,17] The former material (PDA = partially dehydroxylated alumina) has a surface area of ca. 160 m^2/g (by BET techniques) and a coverage of ca. 4 surface OH groups (weak Brønsted acid), 5.5 surface O^{2-} groups (strong Lewis base), and 5.5 exposed Al^{3+} (strong Lewis acid) sites per 100 Å^2.[8,10a,17] The latter alumina (DA = dehydroxylated alumina) has a comparable surface area, contains significant amounts of the orthorhombic δ polymorph, and has a surface composed mainly of O^{2-} and exposed Al^{3+} ions, with ca. 0.12 residual OH units per 100 Å^2.[8,10a,17]

$Cp'_2M(CH_3)_2$. Surface Reaction Pathways. Initial experiments established that $Cp'_2M(CH_3)_2$ compounds are rapidly adsorbed from hydrocarbon solutions onto PDA or DA. This transformation is particularly striking for $Cp'_2U(CH_3)_2$ in pentane—upon slurrying with alumina, the dark red solutions are rapidly decolorized and the alumina becomes bright orange in color. There is no evidence that the adsorbed $Cp'_2U(CH_3)_2$ can be removed by prolonged extraction with toluene or pentane. Assuming that Cp′H adsorption on $Cp'_2M(CH_3)_2$-covered alumina is unimportant under the reaction conditions, quantitative solution spectrophotometric experiments (see Experimental Section for details) indicate that for typical $Cp'_2M(CH_3)_2$ coverages on DA, less than ca. 0.15% of available Cp′ ligands are protolytically liberated into the solvent as Cp′H upon room temperature activation, while on PDA, this quantity is on the order of ca. 2.5%. The degree to which Cp′ ligands might be lost from the actinide centers but still firmly retained on the surface is more difficult to assess. However, both the known solution chemistry of the Cp'_2MR_2 complexes[4,12] and the surface NMR results[7] argue that such processes are not competitive with transformations occurring at M–C and M–H σ bonds.

During activation of adsorbed $Cp'_2U(CH_3)_2$ and $Cp'_2Th(CH_3)_2$ in flowing helium or hydrogen at temperatures up to 150 °C, the only compound that is evolved in detectable quantities is methane. Significantly, the amount of H_2 liberated by $Cp'_2U(CH_3)_2$ is less than 0.01 equiv (H_2/U), arguing that the bulk of the uranium centers remain in the 4+ oxidation state. Only during activation in flowing hydrogen at temperatures in excess of 200 °C are higher hydrocarbons, i.e., C_2H_6 and C_3H_8, noted. These are presumably formed by decomposition of Cp′. In Table I are shown data from a typical activation experiment carried out over a range of conditions. Here an abbreviation of the form He,0°,1 indicates

(19) (a) Bruno, J. W.; Marks, T. J.; Morss, L. R. *J. Am. Chem. Soc.* **1983**, *105*, 6824–6832. (b) Sonnenberger, D. C.; Marks, T. J.; Morss, L. R. *Organometallics*, in press.

(20) (a) Fagan, P. J.; Maatta, E. A.; Marks, T. J. *ACS Symp. Ser.* **1981** *No. 152*, 53–78. (b) Fagan, P. J.; Manriquez, J. M.; Marks, T. J.; Day, V. W.; Vollmer, S. H.; Day, C. S. *J. Am. Chem. Soc.* **1980**, *102*, 5393–5396. (c) Fagan, P. J.; Manriquez, J. M.; Marks, T. J.; Vollmer, S. H.; Day, C. S.; Day, V. W. *J. Am. Chem. Soc.* **1981**, *103*, 2206–2220. (d) Maatta, E. A.; Marks, T. J. *J. Am. Chem. Soc.* **1981**, *103*, 3576–3578.

(21) (a) Sonnenberger, D. C.; Mintz, E. A.; Marks, T. J. *J. Am. Chem. Soc.* **1984**, *106*, 3484–3491. (b) Moloy, K. G.; Marks, T. J. *J. Am. Chem. Soc.* **1984**, *106*, 7051–7064.

(22) Fagan, P. J.; Moloy, K. G.; Marks, T. J. *J. Am. Chem. Soc.* **1981**, *103*, 6959–6962.

(23) Katahira, D. A.; Moloy, K. G.; Marks, T. J. *Organometallics* **1982**, *1*, 1722–1726.

(24) Duttera, M. R.; Suzuki, H.; Marks, T. J., manuscript in preparation.

(25) Fagan, P. J.; Manriquez, J. M.; Marks, T. J.; Day, C. S.; Vollmer, S. H.; Day, V. W. *Organometallics* **1982**, *1*, 170–180.

(26) For authoritative reviews on the surface chemistry and structure of alumina, see: (a) Beránek, L.; Kraus, M. In "Comprehensive Chemical Kinetics"; Bamford, C. H., Tipper, C. F. H., Eds.; Elsevier: Amsterdam, 1978; pp 263–398. (b) Benesi, H. A.; Winquist, B. H. C. *Adv. Catal.* **1978**, *27*, 97–182. (c) Knözinger, H.; Ratnasamy, P. *Catal. Rev.—Sci. Eng.* **1978**, *17*, 31–70. (d) Lippens, B. C.; Steggerda, J. J. In "Physical and Chemical Aspects of Adsorbents and Catalysts"; Linsen, B. G., Ed.; Academic Press: London, 1970; Chapter 4.

activation in flowing helium at 0 °C for 1 h. It can be seen that the rate of formation of methane decreases with time and, on DA, at 100 °C in He, the total CH_4/M yield is much less than the available CH_3/M in the starting complexes and less than the total available surface hydroxyl ($OH/M \approx 0.4$). Experiments involving activation under H_2 will be discussed in a following section. In general, $Cp'_2U(CH_3)_2$ and $Cp'_2Th(CH_3)_2$ exhibit similar behavior with regard to methane yields. Minor variations probably result from differences in loading, degree of alumina dehydroxylation (vide infra), and possible impurities present during catalyst preparation and activation.

A set of deuterium labeling experiments at loadings $\lesssim 1.0$ $Cp'_2M(CH_3)_2/100$ Å^2 DA was next devised to delineate the pathways for methane evolution, both as a function of alumina hydroxylation, M, and activation conditions (heating under a He flow at various temperatures). Experiments with $Cp'_2M(CH_3)_2$, $Cp'_2M(CD_3)_2$, PDA, and DA (and deuterated analogues PDA-*d*, DA-*d*) were designed to probe for three methane-evolving pathways, all of which have precedent in homogeneous organoactinide or organotransition-metal chemistry. These are protonolytic[12-15,19] H abstraction from a surface OH (pathway S), H abstraction from a Cp′ ring (pathway R),[27] and H abstraction from another methyl group (pathway M).[28] As depicted without specification as to molecular structure or reaction molecularity in Scheme I, experiments 1, 2, and 3 assay pathways S, M, and R, respectively. Furthermore, this experiment contains a built-in self-consistency test. If Scheme I accurately portrays the methane-evolving chemistry and certain complications are unimportant (vide infra) the sum of the S + R + M methane yields in any set of experiments should equal 100% (1.0 as mole fractions).

Several possible complications must, however, be considered. Independent isotopic exchange between evolved methane and the alumina support would obviously vitiate the pathway assays. Control experiments established that CH_4 exchange with PDA-*d* or DA-*d* is negligible under the reaction conditions (as also implied from the literature[29]). Likewise, other experiments (vide infra) evidence little indication that surface organoactinide species activate exogenous saturated hydrocarbons under the present reaction conditions. Dilution of $M-CD_3$ isotopic labels via exchange with ring-bound protons or pronounced kinetic isotope effects are more difficult to rule out. In regard to the former, we note that evolved methane isotopic distribution patterns adhere closely to the alternatives in Scheme I (CD_4 or CD_3H; CH_3D or CH_4), whereas exchange with the 30 Cp′ methyl hydrogens would likely lead to a broader distribution of labeled methanes. Although there is reasonable precedent for a nonzero kinetic isotope effect in reactions roughly analogous to each of the S, R, or M pathways,[28,30] it is not clear that the C–H/C–D scission processes are rate determining or that there is actual competition among the hydrogen-abstraction pathways. Perhaps the most compelling argument that these effects do not grossly skew the analyses is the self-consistency in reaction pathway yields over a variety of experiments where the partitioning differs considerably.

The results of the labeling experiments are summarized in Table II; agreement with the yields in Table I are reasonable but not excellent. Table II shows that under all conditions, methane yields are far greater on PDA than on DA. Furthermore, pathway S is always dominant on PDA, and the sum of $S + R + M \approx 1.0$. On DA, the behavior of $Cp'_2U(CH_3)_2$ and $Cp'_2Th(CH_3)_2$ is rather similar, but now pathway S is less important. Although R and M are of greater relative importance on DA, absolute R and M yields through He, 100 °C, are nearly identical for $Cp'_2U(CH_3)_2$ on PDA and DA. Again the sum of $S + R + M \approx 1.0$ except where methane yields approach the detection limits. To test whether M products might arise from bimolecular processes, a crossover experiment was conducted in which a mixture of 25.8 μmol of $Cp'_2Th(CH_3)_2$ and 29.9 μmol of $Cp'_2Th(CD_3)_2$ was adsorbed on DA and also activated under He,0°,1; He,25°,1; He,100°,1. Importantly, the products from all three activation periods (CD_4, CHD_3, and CH_4, but negligible CH_3D) were identical with the sum of the isotopic distributions from separate $Cp'_2Th(CH_3)_2$ and $Cp'_2Th(CD_3)_2$ activations. It is thus possible to estimate that the component of pathway M, which is intramolecular, is greater than 95%.

Scheme I. Surface Methane-Evolving Reactions

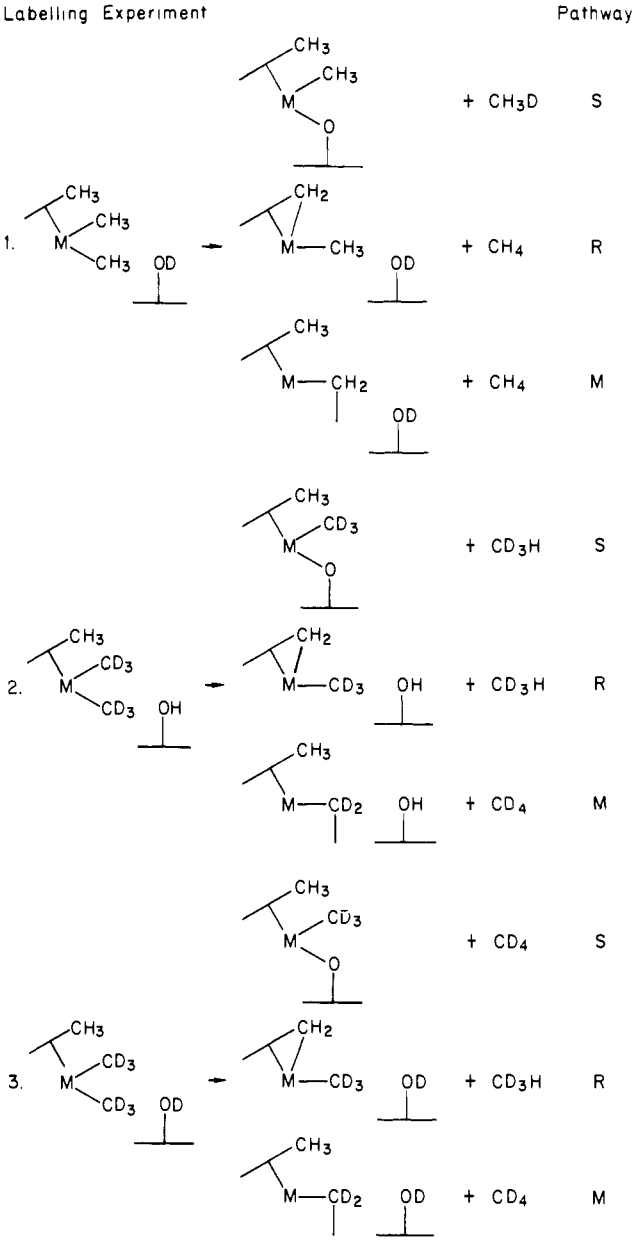

Surface Chemistry of Adsorbed $Cp'_2M(CH_3)_2$-Derived Species. Hydrogenolysis and Metal Hydride Chemistry. The aforementioned labeling experiments raise a number of questions about the nature of surface organometallic species resulting from adsorption

(27) (a) Bruno, J. W.; Smith, G. M.; Marks, T. J., manuscript in preparation. (b) Fendrick, C. M.; Marks, T. J. *J. Am. Chem. Soc.* **1984**, *106*, 2214–2216. (c) Bruno, J. W. Ph.D. Thesis, Northwestern University, Evanston, IL, 1982.

(28) McDade, C.; Green, J. C.; Bercaw, J. E. *Organometallics* **1982**, *1*, 1629–1634 and references therein.

(29) Exchange is observed at longer contact times or higher temperatures: Larson, J. G.; Hall, W. K. *J. Phys. Chem.* **1965**, *69*, 3080–3089.

(30) (a) Matteson, D. S. "Organometallic Reaction Mechanisms"; Academic Press: New York, 1974; pp 120–137 and references therein. k_H/k_D values ranging from 1.0 to 8.0 have been observed for protonolysis of metal–carbon σ bonds. For very polar bonds and oxygen-bound proton donors, the reported values are at the low end of the range. See also: Bencivengo, D. J.; San Fillipo, J., Jr. *Organometallics* **1983**, *2*, 1907–1909. (b) To our knowledge, k_H/k_D has not been measured for H atom abstraction from a Cp′ ligand. For cyclometalation[27] involving $Cp'_2Th[CH_2Si(CH_3)_3]_2$ vs. $Cp'_2Th-[CH_2Si(CD_3)_3]_2$, $k_H/k_D \approx 7$. For $U(C_5H_5)_3R$ vs. $U(C_5D_5)_3R$, RH formation via ring H atom abstraction, $k_H/k_D \approx 8$ (Marks, T. J. *Acc. Chem. Res.* **1976**, *9*, 223–230). (c) For $Cp'_2Ti(CH_3)_2$ vs. $Cp'_2Ti(CD_3)_2$ (pathway M analogue), $k_H/k_D = 2.9$.[28]

Table II. Paths for Methane Formation during Activation of $Cp'_2M(CH_3)_2$ in Helium

Al_2O_3	pathway	$Cp'_2M(CH_3)_2$, μmol	He,0°,1[a]	He,25°,1[a,d]	He,100°,1[a]
		$Cp'_2U(CH_3)_2$			
PDA	S	53.6	0.81	0.72	0.70
PDA	R	18.4	0.12	0.23	0.29
PDA	M	26.0	0.016	0.023	0.012
PDA	S + R + M[b]		0.95	0.97	1.00
PDA	methane[c]		1.20	0.08	0.24
DA	S	18.4	0.45	0.25	0.19
DA	R	45.4	0.45	0.63	0.73
DA	M	20.2	0.07	0.12	0.11
DA	S + R + M[b]		0.97	1.00	1.03
DA	methane[c]		0.12	0.02	0.19
		$Cp'_2Th(CH_3)_2$			
DA	S	47.0	0.69	0.58	0.23
DA	R	45.5	0.31	0.39	0.52
DA	M	50.2	0.03	0.24	0.29
DA	S + R + M[b]		1.03	1.21	1.04
DA	methane[c]		0.16	0.02	0.080

[a] Fraction of methane formed by each pathway, S, R, and M, during indicated activation step. [b] Sum of calculated fraction for each activation step. [c] Mole ratio of methane/complex in each activation step. [d] Small amount of liberated methane limits accuracy.

Table III. Hydrogenolysis Experiments[a]

expt	complex	pretreatment	hydrogen/deuterium treatment	methane/M[b]	product distribution[c] CD_4	CHD_3	CH_2D_2[d]
	$Cp'_2U(CD_3)_2$ (26.0 μmol)/PDA	He,0°,1 He,25°,1 He,100°,1	H_2,100°,1	0.09		0.84	0.16
1	$Cp'_2U(CD_3)_2$ (21.6 μmol)/DA	He,0°,1 He,25°,1 He,100°,1	H_2,100°,1	0.27	0.015	0.99	
2	$Cp'_2U(CD_3)_2$ (45.4 μmol)/DA-*d*	He,0°,1 He,25°,1 He,100°,1	H_2,100°,1	0.23	0.046	0.85	0.11
3	$Cp'_2U(CD_3)_2$ (47.1 μmol)/DA-*d*	He,0°,1	D_2,25°,1 D_2,100°,1	0.17 0.30	0.86 0.76	0.14 0.24	
4	$Cp'_2Th(CD_3)_2$ (16.6 μmol)/DA	He,0°,1 He,100°,7	H_2,100°,1	0.17	0.01	0.82	0.17

[a] Experiments numbered according to Scheme II. [b] Yield for H_2/D_2 treatment which always followed He,0°,1;He,25°,1;He,100°,1 except in experiments 3 and 4 where it followed He,0°,1;He,0°,1;He,100°,7, respectively. [c] Fraction of each isotopic species formed in H_2/D_2 treatment. [d] Interfering water signal limits accuracy.

and He activation. Table II shows that for $Cp'_2U(CH_3)_2$ the cumulative methane yield on PDA (predominantly via pathway S) is on the order of 76% of the available methyl groups. However, it can also be seen that the cumulative methane yield on DA is only ca. 17% of the available methyl groups for $Cp'_2U(CH_3)_2$ and only ca. 13% for $Cp'_2Th(CH_3)_2$. To probe the fate of the remaining M–CH_3 functionalities, hydrogenolysis (c.f., eq 2[4,12]), and surface NMR spectroscopic investigations[7] were carried out. The data in Table I typify H_2,100°,1 methane yields found on DA—the methane yield is approximately doubled, but the cumulative yield is still far below stoichiometric. Labeling experiments (Scheme II, Table III) provide more information on the source of methane from $Cp'_2U(CD_3)_2$ and $Cp'_2Th(CD_3)_2$ at H_2,100°,1. First, essentially no CH_4 is produced by H_2,100°,1 activation, nor CH_3D by D_2,100°,1[31a] activation. Thus, there is no evidence for significant hydrogenolysis of the methyl groups of Cp′ under these conditions. Second, on PDA H_2,100°,1, there is considerably less methane produced than on DA under identical conditions (vide infra); however, the cumulative yield on PDA now reaches 81% of the available methyl groups. The bulk of the evolved methane is CHD_3, so pathway M is unimportant; pathways S, R, and hydrogenolysis cannot be distinguished from these data. With $Cp'_2U(CD_3)_2$/DA, the yields of methane from H_2,100°,1 are roughly equal to those from the preceding pretreatment with He. Cumulative yields are on the order of 35% of available methyl functionalities. It can be seen in Scheme II that under the assumptions made for the investigations in Scheme I (vide supra), labeling experiments 1–3 approximately assay the relative importance of pathways S, R, M, and hydrogenolysis (H). Assuming approximate additivity of the various pathways, we find that for $H_2(D_2)$,100°,1, the methane/U yields on DA are roughly on the order of 0.003, 0.01, ≈0.07, and ≈0.2 for M, S, R, and H, respectively (Table III).[31b] Comparison of uranium (experiment 1) with that for thorium (experiment 4, Table III) indicates that both metals behave rather similarly. Thus, the hydrogenolysis experiments strongly argue for the presence of actinide–methyl groups on the surface-bound species, but only ca. 25% are accessible for cleavage by H_2,100°,1.

The occurrence of pathway H suggests the presence (at least transitory) of actinide–hydride functionalities on the surface. Considering the importance of M–H functionalities to the catalysis results (vide infra) and the possibility that processes analogous to S and R pathways could destroy surface organoactinide hydrides, assays of active M–H groups were carried out by titrating with CH_3Cl (cf. eq 5). Complexes $Cp'_2Th(CH_3)_2$ and $Cp'_2U(CH_3)_2$ were adsorbed on DA by the usual procedure and were then pretreated by He,0°,1;H_2,100°,1;He,100°;He,25°. The latter two steps were conducted to sweep out any desorbable H_2 and CH_4. When methane in the helium stream had fallen to 0.1 μmol h^{-1}, a pulse of methyl chloride (120–160 μmol) was injected at 25 °C, and the evolved products were collected and analyzed by GC. For 49.4 μmol of $Cp'_2Th(CH_3)_2$, the pretreatment conditions liberated methane/Th = 0.34; exposure to CH_3Cl liberated an

(31) (a) Minimal exchange of surface OH groups with D_2 is expected under these relatively mild conditions.[10] (b) The somewhat different activation conditions of experiment 3 limit the accuracy of the R pathway assay. However, the assay of pathway H in experiment 3 should be reasonably accurate since CD_4 evolution via the M pathway is invariably small (cf. experiment 1 and Table II) and not reasonably expected[4,12] to be accelerated by H_2.

Scheme II. Surface Methane-Evolving Hydrogenolysis Pathways

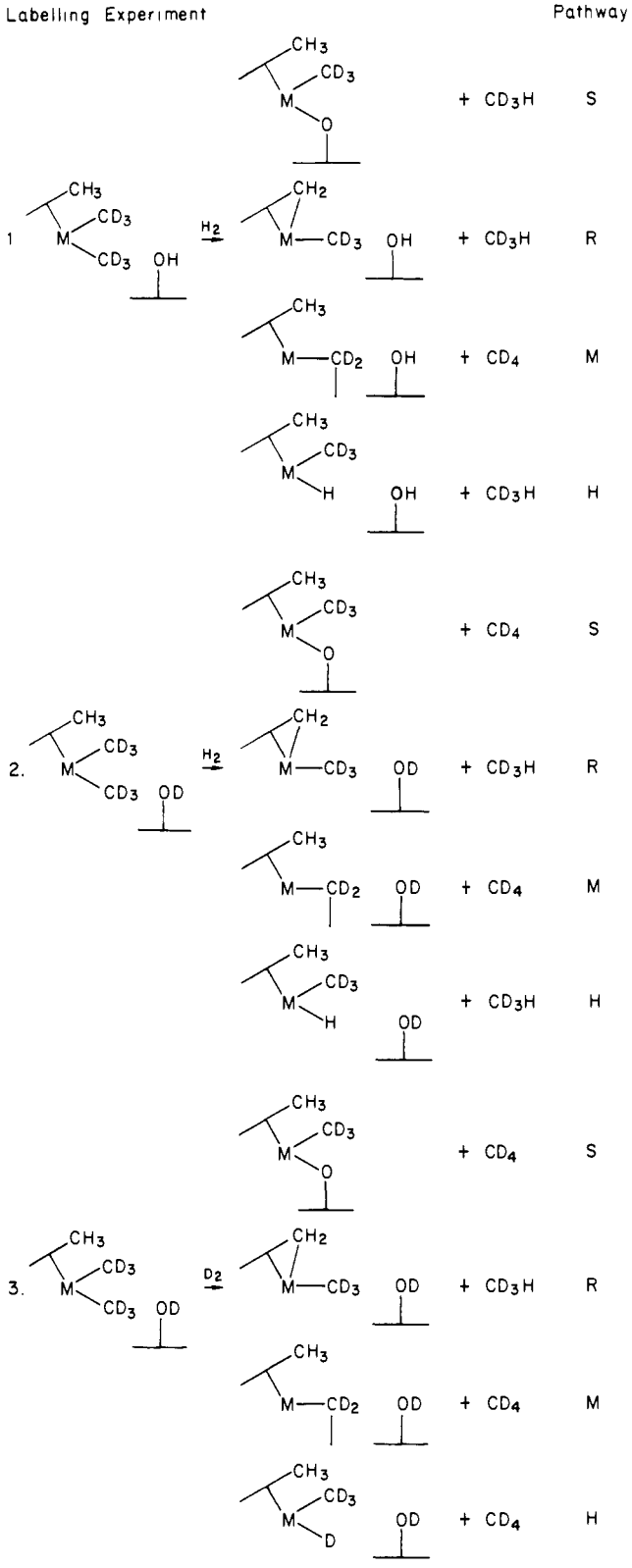

additional methane/Th = 0.020. For 23.1 μmol of $Cp'_2U(CH_3)_2$, pretreatment evolved 0.53 methane/U; exposure to CH_3Cl liberated an additional 0.032 methane/U. These results argue that the quantity of M–H chemically accessible to CH_3Cl is small considering the extent of the M–CH_3 hydrogenolysis pathway.

Surface Chemistry of Adsorbed $Cp'_2M(CH_3)_2$-Derived Species. Alumina-Stabilized Alkylidenes. One of the most interesting results of the surface reaction pathway analysis is the observation of reaction mode M. This process can be interpreted as the intramolecular abstraction of a methyl hydrogen atom by another methyl group. For $Cp'_2U(CH_3)_2$/DA, this pathway accounts for ca. 10% of the evolved methane (Table II, 0.032 CH_4/U out of a total of 0.33 CH_4/U). For $Cp'_2Th(CH_3)_2$/DA, this pathway represents ca. 13% of the evolved methane (Table II, 0.032 CH_4/U out of a total of 0.33 CH_4/U). For $Cp'_2Th(CH_3)_2$/DA, this pathway represents ca. 13% of the evolved methane (Table II, 0.033 CH_4/Th out of a total of 0.26 CH_4/Th). Considering the environment in which this transformation occurs, an interesting analogy of the surface reaction products to the group 4 aluminum-stabilized alkylidene complexes of Tebbe, Grubbs, et al. (D, E) is suggested.[32,33] Examination of this hypothesis was carried out by quantitatively testing the adsorbed organoactinides for alkylidene transfer[32-34] and olefin metathesis[32,33] activity.

Table IV. Reaction of 100-μmol Pulses of Acetone at 25 °C with $Cp'_2M(CH_3)_2$/DA

pulse[a]	1	2	3	total
25.1 μmol of $Cp'_2U(CH_3)_2$/DA; He,0°,1;He,100°,1				
isobutylene, μmol	0.118	0.031	0.012	0.161 (0.0064[b])
pentane, μmol	0.028	0.011	0.000	0.039
28.4 μmol of $Cp'_2Th(CH_3)_2$/DA; He,0°,1;He,100°,1				
isobutylene, μmol	0.188	0.063	0.027	0.287 (0.010[b])
methane,[c] μmol	1.35	0.84	0.52	2.71 (0.095[b])
propane, μmol	0.034	0.014	tr[d]	0.048
propylene, μmol	0.021	0.006	tr[d]	0.027
pentane, μmol	0.082	0.040	0.009	0.12

[a] Three successive pulses of acetone were injected. [b] Ratio of hydrocarbon to M. [c] Trapped on SiO_2 gel at −196 °C rather than in an empty tube at −196 °C so as to trap methane. [d] tr = trace.

Table V. Reactions of $Cp'_2M(CH_3)_2$/DA (He,0°,1;He,100°,1) with One 100-μmol Pulse of Acetone at 25 °C

complex	$Cp'_2U(CH_3)_2$	$Cp'_2U(CH_3)_2$	$Cp'_2Th(CH_3)_2$
amt of complex, μmol	25.1	24.2	44.8
isobutylene/M[a]	0.0047	0.0060	0.0085
pentane, μmol	0.078	0.076	0.068

[a] Mol ratio of isobutylene to M.

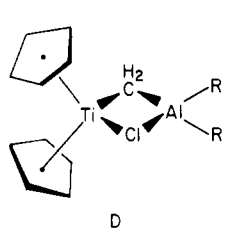

D

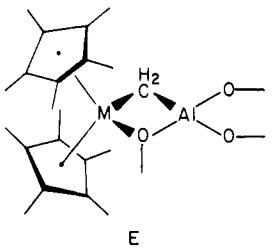

E

To investigate methylidene transfer activity, samples of the adsorbed $Cp'_2M(CH_3)_2$ compounds on DA, activated at He,0°,1;He,100°,1, were treated with 100-μmol pulses of acetone vapor, injected into the helium stream at 25 °C. One molecule of acetone adsorbed per nanometer squared would correspond to 60 μmol of acetone on 0.25 g of alumina. The effluent stream was passed through an empty tube at 78 K, and a released pulse of the trapped material was analyzed by GC. The trapping procedure did not trap methane. Pulses of acetone were also passed over DA prepared as usual and treated with pentane in the usual fashion but without added complex. The results of these acetone experiments are shown in Table IV. In Table V are shown additional experiments in which a single 100-μmol pulse of acetone was employed. In addition, an experiment similar to those in Table

(32) (a) Tebbe, F. N.; Harlow, R. L. *J. Am. Chem. Soc.* **1980**, *102*, 6149–6151. (b) Tebbe, F. N.; Parshall, G. W.; Reddy, G. S. *J. Am. Chem. Soc.* **1978**, *100*, 3611–3613.

(33) (a) Orr, K. C.; deBoer, E. J. M.; Grubbs, R. H. *Organometallics* **1984**, *3*, 223–230. (b) Ott, K. C.; Lee, J. B.; Grubbs, R. H. *J. Am. Chem. Soc.* **1982**, *104*, 2942–2944. (c) Lee, J. B.; Gajda, G. L.; Schaefer, W. P.; Howard, T. R.; Ikariya, T.; Straus, D. A.; Grubbs, R. H. *J. Am. Chem. Soc.* **1981**, *103*, 7358–7361. (d) Howard, T. F.; Lee, J. B.; Grubbs, R. H. *J. Am. Chem. Soc.* **1980**, *102*, 6876–6878.

(34) Pine, S. H.; Zahler, R.; Evans, D. A.; Grubbs, R. H. *J. Am. Chem. Soc.* **1980**, *102*, 3270–3272.

Table VI. Reaction of Propylene with $Cp'_2M(CH_3)_2$/DA (He,0°,1;He,100°,1) at 100 °C

products, μmol	$Cp'_2U(CH_3)_2$, 24.5 μmol	$Cp'_2Th(CH_3)_2$, 44.8 μmol
ethylene	0.012	0.008
propane	0.112	0.045
1-butene	0.004	tr[a]
isobutylene	0.021	0.99
trans-2-butene	0.036	0.005
cis-2-butene	0.016	0.003
trans-2-pentene	0.009	0.018
cis-2-pentene	0.004	tr
2-methyl-2-butene	0.003	tr

[a] tr = trace.

IV was carried out using $Cp'_2U(CD_3)_2$. The isobutylene formed was collected and subjected to mass spectrometric analysis. It was found to be greater than 99% $(CH_3)_2C{=}CD_2$. The isobutylene-evolving processes are readily interpreted in terms of eq 7 and 8. It can be seen in Tables IV and V that isobutylene yields

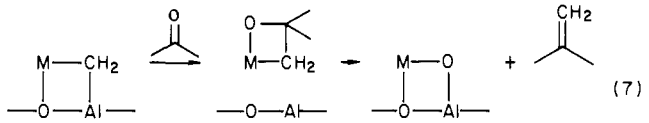

(7)

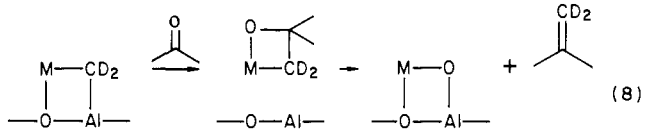

(8)

are on the order of ca. 20% of the methane formed via pathway M for $Cp'_2U(CH_3)_2$ and ca. 30% of the methane formed via pathway M for $Cp'_2Th(CH_3)_2$. In the case of $Cp'_2Th(CH_3)_2$, an assay of evolved methane was also conducted. The yield was significantly higher than that of isobutene. This observation is tentatively interpreted in terms of a previously observed metalation pattern (eq 9).[35] The propane + propylene and pentane detected

$$Cp_3ThCH_3 + CH_3C(=O)CH_3 \rightarrow Cp_3ThOC(=CH_2)CH_3 + CH_4 \quad (9)$$

in this reaction are ascribable to acetone–DA reaction products and solvent, respectively.

Activity of the adsorbed $Cp'_2M(CH_3)_2$ complexes for olefin metathesis was probed by exposing pretreated (He,0°,1;He,100°,1) samples on DA to propylene. First, a pulse of 0.6 μmol of propylene was passed over 55.7 μmol of $Cp'_2Th(CH_3)_2$/DA at 100 °C in helium carrier. Hydrocarbons were removed by a silica gel trap at −196 °C and subsequently analyzed by GC. It was found that 0.014 μmol of methane, 0.01 μmol each of ethylene and propane, and about 0.003 μmol each of isobutylene, 1-butene, *trans*-2-butene, *cis*-2-butene, and pentane had been produced. In view of these low yields, static experiments were run in which a 2-μmol pulse of propylene was isolated in the reactor held at 100 °C for 1 h, helium flow was restored, and the hydrocarbons were caught in an empty trap at −196 °C. This procedure does not trap methane. Some mixing was effected by alternately cooling and warming two U-tubes, which had been inserted on each side of the reactor. A blank experiment was run in which DA was prepared in situ and treated as described under reaction with acetone. Products were pentane (0.020 μmol) and traces of propane but no butenes or butanes. The additional hydrocarbons collected in the $Cp'_2M(CH_3)_2$/DA metathesis experiments are set out in Table VI. No isobutane was detected. To test lifetime for metathesis activity, three successive experiments were run at 100 °C on $Cp'_2Th(CH_3)_2$/DA activated in the usual manner. By the third pulse, olefin product yields had decreased to ca. 25% of the yields in the first pulse. In a similar experiment with only two pulses, increasing the temperature to 150 °C for the second pulse resulted in a modest increase in olefin yield.

(35) Seyam, A. M.; Marks, T. J., unpublished observations.

Table VII. Effect of Temperature of Activation on N_t in the Hydrogenation of Propylene at −63 °C on 11.9 μmol of $Cp'_2U(CH_3)_2$ on 0.25 g of DA

activation[a]	H_2,0°,1	H_2,100°,1	H_2,150°,1
flow rate[b]	77	154	146
conversion[c]	0.75	0.57	0.62
N_t, s^{-1} [d]	0.58	0.89	0.92

[a] The activations were conducted in sequence with a hydrogenation run following each activation. [b] Rate of flow of $H_2 + C_3H_6$ (4.68:1) in cm^3 min^{-1}. [c] Fraction of propylene hydrogenated. [d] After about 1 h.

Table VIII. Hydrogenation of Propylene on Supported $Cp'_2U(CH_3)_2$

μmol[a]	CH_4/U[b]	activation[c]	conversion	N_t, s^{-1}	CO/M[d]
		$Cp'_2U(CH_3)_2$/DA, −63 °C			
11.9	0.10	H_2,150°,1	0.62	0.92	0.019
19.5	0.11	He,100°,1	0.97	0.89	
13.8	0.17	H_2,100°,1	0.97	0.96	
18.8	0.14	He,100°,1			0.019
10.2	0.29	H_2,150°,1	0.50	0.45	
37.6	0.15	H_2,100°,1	1.00	>0.47	0.030
11.2	0.34	H_2,0°,1	0.42	0.37	0.016[e]
9.5	0.59	H_2,100°,1	0.15	0.15	
12.3	0.70	H_2,100°,1	0.08	0.06	
		$Cp'_2U(CH_3)_2$/PDA, −47 °C			
7.4	1.10	H_2,100°,1	0.001	0.001	
13.8	1.12	H_2,100°,1	0.005	0.002	
14.7	1.42	H_2,100°,1	0.02	0.007	
		$Cp'_2U(CH_3)_2/SiO_2$, −47 °C			
10.8[f]		H_2,100°,1	0.000	0.000	
19.0[g]	1.22	H_2,100°,1	0.000	0.000	

[a] μmol of complex on 0.25 g of Al_2O_3. [b] Amount of CH_4 liberated during He,0°,1, mol per mol of U. [c] Activation subsequent to catalyst preparation, He,0°,1. [d] Amount of CO adsorbed per atom of uranium at 25 °C after hydrogenation. Subsequent rate of hydrogenation was drastically reduced. [e] After H_2,100°,1 following the hydrogenation run. [f] Davison grade 62 silica gel, first washed with 0.1 M HNO_3 and then with H_2O and then pretreated in situ at He,400°,2. N_t was 0.05 s^{-1} at 25 °C. [g] The SiO_2 of footnote *f* was further pretreated O_2,500°;H_2,500°;He,500°, cool in He.

Catalysis with Adsorbed $Cp'_2M(CH_3)_2$ Species. Propylene Hydrogenation as a Model Reaction. Studies of propylene hydrogenation, catalyzed by adsorbed $Cp'_2M(CH_3)_2$ species that had been subjected to various activation conditions, were carried out as described in the Experimental Section. To keep conversions below 100% for most activation procedures, when using the maximum possible hydrogen flow rate (160 cm^3 min^{-1}) and the minimum practical catalyst loadings, it was necessary to operate at −63 °C during hydrogenation runs. Below this temperature, filling of the catalyst pores with liquid propylene becomes likely. For these reasons, the turnover frequencies (N_t) reported in this work (propylene molecules hydrogenated per actinide atom per second) are most useful for intercomparing relative rates.

In Table VII are shown the results of some typical propylene hydrogenation experiments as a function of activation conditions. Although the effect is not major, it can be seen that N_t increases slightly with the temperature of H_2 pretreatment. However, in a separate experiment it was found that while 10.2 μmol of $Cp'_2U(CH_3)_2$/DA gave after H_2,100°,1 $N_t = 0.45$ s^{-1}, subsequent activation at H_2,200°,1 gave $N_t = 0.13$ s^{-1}. Thus, very high activation temperatures result in diminution of N_t. The final pretreatments, He,100°,1 and H_2,100°,1, led to nearly the same steady-state catalytic activities. The length of activation times does not appear to have a very large effect upon N_t. Thus, the catalyst prepared in Table I gave $N_t = 0.55$ s^{-1} after the final activation. This value is comparable to that for other $Cp'_2U(CH_3)_2$-derived catalysts (cf. Table VIII).

Turnover frequency data for a variety of other propylene hydrogenation experiments with adsorbed $Cp'_2U(CH_3)_2$ or $Cp'_2Th(CH_3)_2$ are compiled in Tables VIII and IX. Several trends are worthy of note. First, hydrogenation activities on PDA are far lower than on DA. Second, the large amount of data in Table VII indicates that there is a general trend for increasing

Table IX. Hydrogenation of Propylene on Supported $Cp'_2Th(CH_3)_2$ at −63 °C

μmol	CH_4/M^a	activation	conversion	N_t, s^{-1}	CO/M^b
		$Cp'_2Th(CH_3)_2$/DA			
32.2	0.10	H_2,100°,1	0.95	0.51	0.021
45.2	0.12	He,100°,1	1.00	>0.40	0.022
16.6	0.08	H_2,100°,1[c]	0.50	0.55	
6.6	0.12	H_2,100°,1	0.18	0.54	0.027
		$Cp'_2Th(CH_3)_2$/PDA			
27.6	0.59	H_2,100°,1	0.027	0.005	0.002[d]

[a] CH_4 liberated per atom of actinide during He,0°,1. [b] CO adsorbed at 25 °C per atom of thorium. [c] On catalyst of Table I. [d] Indistinguishable from zero to within experimental accuracy.

CH_4 yields during activation to parallel decreasing N_t values. The greatest range of catalyst loadings for identical activation conditions is explored in Table IX. For a ca. 5-fold range in the quantity of supported $Cp'_2Th(CH_3)_2$, N_t is essentially unchanged. This result and those to be discussed below suggest that mass transport effects are likely to be rather minor in these experiments. Lastly, catalytic results with $Cp'_2U(CH_3)_2$ supported on silica gel are reported in Table VIII. Activity for propylene hydrogenation is low.

A series of isotopic tracer experiments was conducted in which pulses of propylene were injected into deuterium flowing over $Cp'_2Th(CH_3)_2$/DA (pretreatment: He,0°,1;D_2,100°,1) or $Cp'_2U(CH_3)_2$/DA (pretreatment: He,0°,1;He,100°,1) at 0 °C. Conversions to propane were 100%, and it was found mass spectrometrically that ≳90% of the propane was propane-d_2. It was also found in a blank experiment that propane pulses over pure DA underwent no detectable isotopic exchange with the deuterium carrier at 25, 50, or 100 °C.

For reference, the rate of hydrogenation of propylene on 80–100 mesh 0.78% Rh/Davison grade 62 silica gel was measured at −63 °C. The catalyst was prepared by ion exchange with $Rh(NH_3)_5(OH_2)^{3+}$ and reduction in hydrogen at 370 °C. It had a percentage of exposed Rh of 58% as measured by hydrogen chemisorption at 25 °C. It was pretreated in situ with O_2,300°,0.5;H_2,300°,0.5 and cooled in H_2 to −63 °C. The rate of hydrogenation of propylene declined somewhat initially, but was constant from 95 to 155 min, N_t = 27 s^{-1} per Rh_s.

To date, it has not been possible to obtain normal kinetic data on the $Cp'_2M(CH_3)_2$-catalyzed propylene hydrogenation. All unpoisoned catalysts are so active that practicable amounts of complex at practicable flow rates give conversions of 50% or greater. Such high activity prevents operation in the differential regime. Further, of course, activation energies could not be obtained. However, some kinetic information was obtained for poisoned or deactivated catalysts. One such catalyst consisted of 19.6 μmol of $Cp'_2U(CH_3)_2$ on DA—the low activity was apparently a consequence of improperly purified pentane. The flow rate of C_3H_6 + H_2 was varied, and N_t (0.018 s^{-1}) was found to be constant over a range of conversions of 0.025 to 0.15. In an experiment with 12.1 μmol of $Cp'_2U(CH_3)_2$ (on DA) which exhibited an initial N_t of 0.92 s^{-1} and which had become deactivated by several days use, N_t was approximately constant at 0.17 s^{-1} over a range of conversions of 0.15–0.85. These results suggest that, at least for a deactivated catalyst, the hydrogenation reaction is near zero order in olefin. Any effect of change in pressure of hydrogen would not have been detectable within the limits of experimental reproducibility.

The question of the intrusion of mass transport effects can be approached using the Wei–Prater criterion.[36] Assuming that D_{eff} is 0.1 times that of the bulk diffusion coefficient of propylene,[36] a Wei–Prater number ca. 0.5 is obtained for the first entry in Table VIII. Thus, the values of N_t in Tables VIII and IX should be free of the effects of concentration gradients of propylene in the catalyst pores unless there are severe local concentration gradients in the pores resulting from the very high rates at the small fraction of adsorbed molecules of complex that become converted to catalytic sites. On the basis of the Wei–Prater criterion, hydrogenations on the more active Rh/SiO_2 are marginal with respect to the intrusion of the effects of mass transport. The question of the intrusion of the effects of heat transport is less clear, particularly in the case of the Rh catalyst just mentioned.

Poisoning of $Cp'_2M(CH_3)_2$-Catalyzed Propylene Hydrogenation by Carbon Monoxide. The injection of pulses of carbon monoxide at 25 °C has a dramatic effect on the hydrogenation activity of $Cp'_2M(CH_3)_2$/DA catalysts. General information on the chemical systematics is given in Tables VIII, IX, and XII and in the discussion which follows. In all cases, CO/M adsorption ratios are rather small, indicating that only a fraction of the actinide sites is reactive. A blank experiment on 0.25 g of DA impregnated with pentane and pretreated in the usual manner indicated that CO adsorption on DA—only ca. 0.03 μmol—is not a major constituent of the adsorption.[37] The quantity of CO adsorbed by the supported organometallics is approximately the same when measured immediately after activation as after a preliminary hydrogenation run at −63 °C. In general, if catalyst activation was in hydrogen, CO adsorption was measured from a hydrogen carrier, while if catalyst activation was in helium, CO adsorption was measured from helium. It can be seen that CO/M ratios are rather similar for the two activation modes. Adsorptions of carbon monoxide were measured on two samples of about 16 μmol of $Cp'_2Th(CH_3)_2$/DA, one activated in H_2,100°,1 and the other in He,100°,1. The hydrogen was then changed to helium and the helium to hydrogen and the adsorption of a second pulse of carbon monoxide was measured. The additional amounts of carbon monoxide adsorbed were small, but essentially identical within the experimental error.

When hydrogenation experiments at −63 °C were conducted immediately after CO adsorption from either helium or hydrogen at 25 °C, catalytic activity was found to be markedly depressed. In the case of CO adsorption from hydrogen, N_t values fell to ≲10% of normal values and remained at this level. For example, in experiments with 6.6 and 32.2 μmol of $Cp'_2Th(CH_3)_2$/DA in Table IX and 11.2 μmol of $Cp'_2U(CH_3)_2$/DA in Table VIII, the catalysts were saturated with carbon monoxide in hydrogen at 25 °C and hydrogenations were run at −63 °C. N_t values after poisoning were 0.03, 0.01, and 0.05 s^{-1}, respectively, and there was no increase in activity with time on stream. These activities were less than 10% of those before treatment with carbon monoxide. One immediate conclusion that follows from these results is that the bulk of the hydrogenation catalysis is occurring at a small fraction of the adsorbed organoactinide molecules.

Although carbon monoxide appears to adsorb on the same sites from helium and from hydrogen streams and both procedures poison hydrogenation, different adsorbed species seem to result. Although neither adsorbed species desorbs significantly in flowing hydrogen or helium, at 25 °C, adsorbed CO is partly removed by hydrogen plus propylene at −63 °C from catalysts saturated with carbon monoxide in helium but, as already discussed, not from catalysts saturated with carbon monoxide in hydrogen. Thus, the activity of catalysts poisoned from flowing helium is slowly recovered. An example is provided by the experiments with 18.8 and 37.6 μmol of $Cp'_2U(CH_3)_2$/DA in Table VIII. Adsorption of carbon monoxide in helium at 25 °C was measured on the 18.8-μmol sample directly after activation, on the 37.6-μmol sample after a hydrogenation run at −63 °C followed by He,−63°,0.5. Hydrogenation runs were then effected at −63 °C. N_t's (s^{-1}) and (conversions) at 5 min on stream and 90 min on stream were as follows: for 37.6 μmol, 0.05 (0.18) and 0.42 (0.91) and, for 18.8 μmol, 0.11 (0.11) and 0.31 (0.31).

Adsorbed carbon monoxide also inhibited the reaction with acetone. Thus, adsorption of carbon monoxide was measured on 18.2 μmol of $Cp'_2U(CH_3)_2$, He,100°,1. The ratio CO/U was

(36) Butt, J. B. "Reaction Kinetics and Reactor Design"; Prentice-Hall Inc.: Englewood Cliffs, NJ, 1980; pp 368, 388.

(37) Adsorption of CO at 25 °C on DA directly (without exposure to and evaporation of pentane) was larger, about 0.3 μmol per 0.25 g. Some pentane remained adsorbed on DA after He,0°,1;He,100°,1 during catalyst preparation and activation. Some of this is displaced by acetone at 25 °C in the cases of $Cp'_2U(CH_3)_2$/DA and $Cp'_2Th(CH_3)_2$/DA.

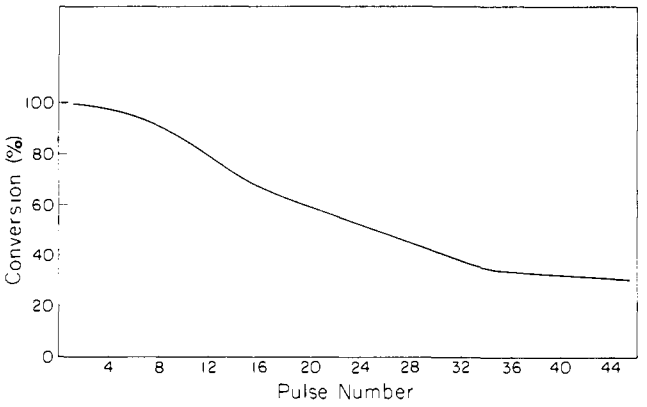

Figure 2. Diagram showing the decline in ethylene polymerization activity by $Cp'_2U(CH_3)_2$/DA (14.7 μmol, He,0°,1;H_2,100°,1,He,25°,18) as a function of 14.7 μmol of ethylene pulse number.

Table X. Polymerization of Ethylene on $Cp'_2Th(CH_3)_2$/DA and $Cp'_2U(CH_3)_2$/DA Using 20 Successive Pulses of Ethylene

	$Cp'_2Th(CH_3)_2$		$Cp'_2U(CH_3)_2$	
complex, μmol	27.3	30.1	23.3	22.3
activation[a]	He,100°,1	H_2,100°,1 He,25°,17	He,100°,1	H_2,100°,1 He,25°,17
C_2H_4/M	19	19	17	17
conversion in 20th pulse	0.85	0.86	0.69	0.72

[a] Activation subsequent to He,0°,1.

0.018. A 100-μmol pulse of acetone was then passed over the catalyst at 25 °C. The micromoles of product and product/U were as follows: propylene, 0.019 and 0.0010; isobutylene, 0.019 and 0.0013. The micromoles of propylene formed was little changed by preliminary adsorption of carbon monoxide (compare Table IV), but that of isobutylene was reduced to $^1/_3$ to $^1/_4$ of the value in the absence of treatment with carbon monoxide.

Catalysis with Adsorbed $Cp'_2M(CH_3)_2$ Species. Butene Isomerization and Ethylene Polymerization. A 0.20-μmol pulse of 1-butene in helium passed at 25 °C over 17.9 μmol of $Cp'_2U(CH_3)_2$/DA activated in He,100°,1, was about 50% isomerized, and the *trans*-2-butene/*cis*-2-butene ratio was ca. 3.6. On DA alone under similar conditions, the trans/cis ratio was ca. 2.0. On 55.7 μmol of $Cp'_2Th(CH_3)_2$/DA activated in He,100°,1, the conversion of a 1.6 μmol pulse of 1-butene in helium was 2% at 0 °C. A pulse was then passed at 50 °C. The conversion was 13% and the 1-butene/*trans*-2-butene ratio was about 12. Small amounts of pentane and butane and traces of propane, propylene, methane, and ethylene were also found. Further studies would be required to separate fully actinide and support contributions to these rather slow isomerizations.

Ethylene polymerization was studied by injecting a series of ethylene pulses into helium flowing over the catalyst at 25 °C. The percentage of each pulse of ethylene that was adsorbed vs. pulse number is shown in Figure 2 for an experiment with $Cp'_2U(CH_3)_2$. The initial adsorption of ethylene was nearly 100%, but even at the 45th pulse the adsorption was 30% of the pulse. The total loss in ethylene per atom of uranium, C_2H_4/U, was 42. Table X shows that $Cp'_2U(CH_3)_2$/DA and $Cp'_2Th(CH_3)_2$/DA have similar activities for ethylene polymerization. Control experiments verified that DA is not an ethylene polymerization catalyst. The properties of the polyethylene deposited on the catalyst were not examined.

Carbon monoxide partially inhibited polymerization as shown in Table XI. Except for the experiment with 18.4 μmol of $Cp'_2U(CH_3)_2$, a polymerization experiment was conducted and carbon monoxide was injected into helium passing over the catalyst at 25 °C so as to measure the adsorption of CO. A further pulse of ethylene was then injected. Values of CO/M were similar to those reported in Tables VIII and IX.

Catalytic Experiments with Other Organoactinide Complexes. To explore the effects of coordinative unsaturation and available reactive metal–ligand functionalities, survey catalytic experiments were also carried out with Cp_3UCH_3, $Cp_3Th(n\text{-}C_4H_9)$, $Cp'_2U(CH_3)Cl$, $Cp'_2Th[CH_2C(CH_3)_3]_2$, $[Cp'_2Th(\mu\text{-}H)H]_2$, and $Cp'Th(CH_2C_6H_5)_3$. The results for propylene hydrogenation are summarized in Table XII. It can be seen that the coordinatively rather saturated[4,14,15] Cp_3MR complexes are relatively inactive catalysts for propylene hydrogenation under all pretreatment conditions explored. Remarkably, however, $Cp_3Th(n\text{-}C_4H_9)$ still exhibits modest activity after pretreatment at temperatures as high as 350 °C for 2 h. Neither of the Cp_3MR complexes exhibit detectable ethylene polymerization activity at room temperature.

Table XI. Effect of Carbon Monoxide on the Polymerization of Ethylene

	$Cp'_2U(CH_3)_2$/DA	$Cp'_2Th(CH_3)_2$/DA	$Cp'_2U(CH_3)_2$/DA
complex, μmol	18.4	30.1	14.7
activation[a]	He,100°,1	H_2,100°,1; He,25°,17	H_2,100°,1 He,25°,17
conversion in last pulse[b]	not run	0.77	0.31
C_2H_4/M[c]	not run	23	42
CO/M[d]	0.023	0.032	0.024
conversion in next pulse[e]	0.63	0.50	0.09

[a] Subsequent to He,0°,1. [b] Conversion in the last pulse in a sequence of pulses of ethylene. [c] Total loss in C_2H_4 in the sequence of pulses. [d] CO adsorption at 25 °C from helium after the sequence of pulses of ethylene. [e] Conversion in the first pulse of ethylene following adsorption of CO.

Table XII. Hydrogenation of Propylene by Various Organoactinide Complexes Supported on DA

μmol[a]	activation[b]	conversion	N_t, s^{-1}	CO/M[c]	N_t', s^{-1}
		Cp_3UCH_3			
25.0	H_2,100°,1	0.000	0.000		
			0.005 (25 °C)		
		$Cp_3Th(n\text{-}C_4H_9)$			
13.8	He,100°,1	0	0.00 (−63, 0 °C)		
		0.19	0.075 (100 °C)		
24.2	He,100°,1	0	0.00 (−63, 0 °C)		
			0.06 (100 °C)		
	H_2,150°,1		0.10 (100 °C)		
			0.172 (150 °C)		
	H_2,200°,1		0.30 (100 °C)		
			0.19 (200 °C)		
	H_2,250°,2		0.40 (100 °C)		
			0.17 (250 °C)		
	H_2,350°,2		0.36 (100 °C)		
			0.13 (350 °C)		
		$Cp'_2U(CH_3)Cl$			
53.8[d]	H_2,100°,1	0.19	0.02		
27.2[e]	H_2,100°,1	0.04	0.03	0.009	0.004
		$Cp'_2Th[CH_2C(CH_3)_3]_2$			
28.5	He,100°,1	0.99	>0.7	0.015	0.04
10.0	He,100°,1	0.62	0.9	0.05	
		$[Cp'_2Th(\mu\text{-}H)H]_2$[f]			
12.1	H_2,100°,0.25[g]	0.28	0.44		
26.8	H_2,100°,1	1.00	>0.66	0.085	0.009
10.7	He,0°,1[h]	0.065	0.40		
		$Cp'Th(CH_2C_6H_5)_3$			
8.0	He,130°,1	1.00	>3.0	[i]	

[a] μmol of complex on 0.25 g of Al_2O_3. [b] Activation subsequent to catalyst preparation, He,0°,1. [c] Amount of CO adsorbed per atom of actinide at 25 °C after hydrogenation. Subsequent rate of hydrogenation (N_t') was drastically reduced. [d] CH_4/U = 0.07 during He,0°,1 and 0.27 during a subsequent H_2,100°,1. [e] CH_4/U = 0.14 during He,0°,1 and 0.38 during a subsequent H_2,100°,1. [f] Adsorption from benzene solution gives much lower activity than from pentane. Loadings are expressed in μmol of monomer unit. [g] Initial catalyst treatment H_2,0°,1 rather than He,0°,1. [h] H_2/Th yield during He,0°,1 was 0.224. [i] In other experiments, CO/M required to give 90% poisoning was in the vicinity of 0.03.

In regard to variation of $Cp'_2M<$ substituents, it is interesting to note that $Cp'_2U(CH_3)Cl$ yields hydrogenation catalysts of relatively low activity, while the bulky[38] neopentyl ligands of $Cp'_2Th[CH_2C(CH_3)_3]_2$ apparently present no impediment to hydrogenation activity. Indeed, this complex is one of the most active $Cp'_2Th<$ propylene hydrogenation catalysts. In the case of the 28.5-μmol catalyst, the successive adsorptions of three 28.5-μmol pulses of ethylene subsequent to hydrogenation experiments were 95%, 94%, and 92%, implying substantial polymerization activity. In contrast, 54 μmol of $Cp'_2U(CH_3)Cl$ after He,100°,1 was far less effective. Ethylene conversion in the first pulse (40 μmol) was only 30%, and fell to 15% by the fifth pulse; overall through pulse 5, $C_2H_4/U = 0.7$.

The behavior of actinide–hydride functionalities was further investigated in experiments with $[Cp'_2Th(\mu\text{-}H)H]_2$ on DA (Table XII). When adsorbed from pentane solutions (but not benzene solutions), this complex is an active propylene hydrogenation catalyst. During He,0°, at surface $OH/Th \approx 0.8$, the H_2/Th yield of 0.22 is substantially greater than CH_4/Th yields from corresponding $Cp'_2Th(CH_3)_2$ experiments (Table IX). To test the chemical accessibility of Th–H units, the 12.1-μmol hydrogenation catalyst was flushed with He,25°,1 and then treated with a 160-μmol pulse of CH_3Cl at 25 °C. The yield of methane was 1.09 μmol, or $CH_4/Th = 0.09$, which is significantly higher than the 0.020–0.032 CH_4/M ratios obtained with CH_3Cl after hydrogenolysis of $Cp'_2M(CH_3)_2$ (vide supra). $[Cp'_2Th(\mu\text{-}H)H]_2$ is a less effective ethylene polymerization catalyst, and for the complex on DA activated by He,100°,1, conversion in the first pulse was 49%, with conversion falling to zero by the 14th pulse. Overall, conversion was $C_2H_4/Th = 3.6$.

The most active hydrogenation catalyst discovered in this study was $Cp'Th(CH_2C_6H_5)_3/DA$. All samples were activated by He,0°,1;He,130°,1, the higher activation temperature being employed to facilitate desorption of toluene. A UV–visible spectroscopic examination of the material condensed in the −196 °C trap after He,0°,1;He,130°,1 revealed, in addition to pentane, the presence of toluene.[39] The exact toluene/Th ratio has not yet been measured. In an early experiment at −63 °C, 8.0 μmol of $Cp'Th(CH_2C_6H_5)_3$ at 25 cm^3 min^{-1} propylene gave 100% conversion ($N_t > 3.0$ s^{-1}). In the present reaction apparatus, the use of small (ca. 1 μmol) amounts of complex gave poorly reproducible results, presumably owing to poisoning of the small quantities of organometallic complex employed. However, results with the more active samples indicate that N_t is greater than 10 s^{-1} at −63 °C. The problem of heat and mass transport effects is the same as for Rh/SiO_2 (vide supra). The 8-μmol hydrogenation catalyst readily polymerized ethylene, and after 10 pulses ($C_2H_4/Th = 1$), there was 98% conversion in the final pulse.

It is of interest to note that the treatments He,0°,1;He,100°,1 for $Cp'_2Th[CH_2C(CH_3)_3]_2$, He,0°,1;He,130°,1 for $Cp'Th(CH_2C_6H_5)_3$, and H_2,0°,1;H_2,100°,0.25 for $[Cp'_2Th(\mu\text{-}H)H]_2$ led to the liberation of no methane. This supports the conclusion that such treatments do not lead to the liberation of methane from the methyl groups of pentamethylcyclopentadienyl ligand.

The active catalysts shown in Table XII were poisoned by CO in the same manner as those derived from $Cp'_2M(CH_3)_2$. Small CO/M ratios were measured in all cases except $[Cp'_2Th(\mu\text{-}H)H]_2$. Here the ratio was 0.085 and the value of N_t at −63 °C was only 1% of the value prior to poisoning. Subsequent treatment at H_2,100°,1 raised N_t to only 2% of the initial value.

Discussion

From the results of this investigation it is evident that organoactinide/alumina surface chemistry is very rich, reflecting both the ligation of the actinide ion as well as the reactive functionalities available on the PDA or DA alumina surface. For $Cp'_2M(CH_3)_2$ complexes, there is now chemical evidence for surface Al^{3+}-stabilized alkylidene (e.g., E), aluminoxy (e.g., F, G), and $\eta^1{:}\eta^5$-$(CH_3)_4C_5CH_2$ (e.g., H) interactions. Support for schematic

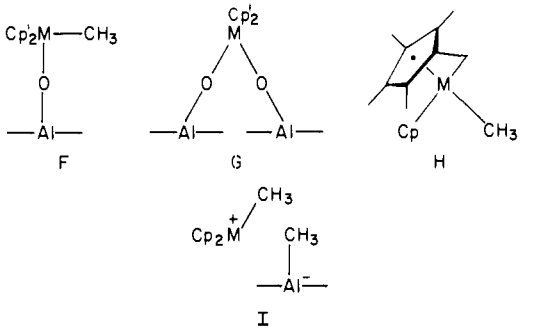

structures F and G is also derived from surface ^{13}C NMR studies.[7] A further role for the coordinatively unsaturated surface Al^{3+} sites of DA follows from the NMR studies which suggest strong interaction of actinide-bound alkyl ligands and by implication hydride ligands, with aluminum centers on the surface (e.g., I). In cases of high surface coverage by OH (PDA) the surface chemistry largely follows pathways leading to species of types F and G. Some η^5-$(CH_3)_5C_5$ protonolysis also occurs, although this pathway is more difficult to quantitate (traces of Cp'H are liberated from the alumina; no species other than Cp'Th can be unambiguously discerned in the NMR[7]). Interestingly, however, pathways leading to species such as E and H are operative under all conditions of surface pretreatment and each to roughly the same absolute degree. There is no evidence that significant quantities of the adsorbed uranium ions attain an oxidation state higher than 4+.

Chemical probes to test the reactivity of the adsorbed $Cp'_2M(CH_3)_2$ molecules reveal that there is a broad range in the reactivity of the $M–CH_3$ functionalities. For example, a rather large proportion of the CH_3 groups remaining on the surface (i.e., not evolved as CH_4) are not readily hydrogenolyzed, despite the high hydrogenolytic reactivity of the $Cp'_2M(CH_3)_2$ compounds in solution (eq 2).[12] In view of the expected properties of the surface species, this observation is not altogether unexpected. Thus, alkoxide ligands as in F are predicted from solution results[12] greatly to depress rates of hydrogenolysis, and coordinatively saturated methyl aluminates (e.g., I) may also be relatively unreactive.[40] In addition, it is conceivable that a number of adsorbed $Cp'_2M(CH_3)_2$ molecules occupy sites with sufficient steric hindrance to retard reaction with any exogenous reagents and/or that other deactivating surface reactions occur. Experiments with acetone indicate that alkylidene species E are active methylene transfer agents. However, the isobutylene yields indicate that not all sites are equally accessible to acetone.

Hydrogenolysis of surface $Cp'_2M(CH_3)_2$ species would reasonably be expected to yield adsorbed organoactinide hydrides, and, indeed, the formation of such species was confirmed by reactions with CH_3Cl. However, the extent of reaction with pulses of CH_3Cl in stoichiometric excess indicate that a significant fraction of the hydride species are not readily accessible to CH_3Cl, possibly for some of the reasons cited above for hydrogenolysis. Experiments with $[Cp'_2Th(\mu\text{-}H)H]_2$ indicate that protolytic reaction with surface OH, presumably generating species analogous to F (CH_3 = H) and G, is also operative for organoactinide hydrides. The NMR results[7] support this conclusion. Again, only a fraction of the hydride centers react with pulses of CH_3Cl at room temperature.

With propylene hydrogenation as a model reaction, it was found that the $Cp'_2M(CH_3)_2/DA$ complexes are highly active catalysts. Indeed, turnover frequencies per atom of M are about 10 times larger than N_t per Pt_s in Pt/SiO_2 at −63 °C (0.05 s^{-1} [41]). Per

(38) (a) Bruno, J. W.; Marks, T. J.; Day, V. W. *J. Organomet. Chem.* **1983**, *250*, 237–246. (b) Bruno, J. W.; Smith, G. M.; Schultz, A. J.; Day, V. W.; Marks, T. J., unpublished results.

(39) Silverstein, R. M.; Bassler, G. C.; Morrill, T. C. "Spectrometric Identification of Organic Compounds", 4th ed.; Wiley: New York, 1981; Chapter 6.

(40) Eisch, J. J. In "Comprehensive Organometallic Chemistry"; Wilkinson, G., Stone, F. G. A., Abel, E. W., Eds.; Pergamon Press: Oxford, 1982; Chapter 6, p 630.

Scheme III

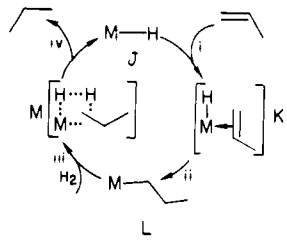

effective catalytic site, as measured by CO poisoning, activated $Cp'_2M(CH_3)_2$/DA gives a rate of propylene hydrogenation ca. 300 times that of a surface atom of Pt. Rhodium is usually considered to be the most active heterogeneous hydrogenation catalyst. We measured N_t per Rh_s on Rh/SiO_2 and found it to be $\sim 27\ s^{-1}$ at −63 °C. In comparison, N_t per Th of $Cp'Th(CH_2C_6H_5)_3$/DA is about $10\ s^{-1}$ at −63 °C, but per active site, about $300\ s^{-1}$. The activity of this complex on DA is thus extraordinary, and all steps in the catalytic cycle must have unusually small activation energies. Thus, despite the aforementioned sluggish reactivity of a high percentage of the adsorbed species with respect to M–C hydrogenolysis (likely an essential component of the catalytic cycle; vide infra) it appears that a small fraction of the sites is highly reactive. That the percentage is small is also confirmed by the CO poisoning experiments, which place an upper limit on this fraction of ca. 2–3%. It is likely that the poisoning reaction involves migratory CO insertion, which in solution is generally irreversible for an actinide–carbon bond (eq 1) but reversible for an actinide–hydrogen bond (eq 2). The complexes $Cp'_2Th[CH_2C(CH_3)_3]_2$ and $[Cp'_2Th(\mu\text{-}H)H]_2$ are also precursors for highly active hydrogenation catalysts, so that a Th–CH_3 functionality is not an absolute necessity. The highest upper limits on the percentage of metal centers that are catalytically active, as deduced from CO poisoning, are found for these latter two complexes to be $Cp'_2Th[CH_2C(CH_3)_3]_2$/DA, ca. 3%, and $[Cp'_2Th(\mu\text{-}H)H]_2$/DA, 8.5%. It is not clear at this time why the reversibility of poisoning varies with precatalyst and CO carrier. The observation that the catalytic behavior of $Cp'_2Th(CH_3)_2$ and $Cp'_2U(CH_3)_2$ is nearly identical argues that shuttling to metal 3+, 5+, or 6+ oxidation states (reductive elimination, oxidative addition), which are not readily accessible to thorium,[4] is not mechanistically important. Although supporting $Cp'_2M(CH_3)_2$ complexes on DA yields highly active hydrogenation catalysts, supporting them on PDA or silica gel does not produce highly active catalysts. Upon impregnation with $Cp'_2M(CH_3)_2$, the latter two systems evolve considerably greater yields of methane; i.e., a higher percentage of precatalytically important (vide infra) M–CH_3 bonds is destroyed or apparently reduced in reactivity (e.g., F, G). Modifying the coordinative saturation about the actinide center also has dramatic consequences for the catalytic activity vis-à-vis the $Cp'_2M(CH_3)_2$/DA systems. Thus, more coordinatively saturated and generally less reactive Cp_3MR compounds yield far less active hydrogenation catalysts under any pretreatment conditions, while the formally less saturated and highly reactive $Cp'Th(CH_2C_6H_5)_3$ complex yields the most active catalyst of all.

A plausible scenario for catalytic olefin hydrogenation by an f-element catalyst, which is in accord with most of the findings of this study, is shown in Scheme III. Here the species in brackets are intermediates or transition states (unspecified). Assuming the metal does not change oxidation state, it can be seen that a hydrogenolyzable M–R or preformed M–H group is a straightforward prerequisite to J. The facility with which steps i and ii occur will reflect, among other factors, the ease with which olefin can be accommodated in the metal coordination sphere. For $Cp'_2Th<$ systems this reaction is very rapid[12] and is exothermic by ca. 15–20 kcal/mol.[19] Step iii involves a "four-center" hydrogenolysis[12,42,43] process, which in $Cp'_2Th<$ systems can be rapid but is depressed by π-donors (e.g., OR) which presumably decrease the electrophilicity of the metal center;[12] hydrogenolysis is exothermic by ca. 15 kcal/mol.[19] In the absence of detailed kinetic data (such studies are planned), it cannot be determined whether olefin insertion or hydrogenolysis in Scheme III is rate controlling for the present systems. In the only f-element system to date where such data are available, 1-hexene hydrogenation by $(Cp'_2LnH)_2$ compounds (Ln = lanthanide), Ln–hexyl bond hydrogenolysis is rate determining.[44] From Scheme III, it can be seen that CO poisoning via migratory insertion could occur at either J or L; the latter reaction is probably slower, but is far more exothermic.[19]

A plausible scenario for ethylene polymerization would be similar to Scheme III, except that sequential olefin insertion into M–C bonds[3,44-46] would occur instead of step iii. In such f-element systems, β-hydride elimination is at a thermodynamic disadvantage vis-à-vis most middle and late first-row transition-metal complexes.[19] The requirements of unsaturation and metal ion electrophilicity (to polarize the coordinated olefin for intramolecular nucleophilic attack) are likely to be similar to those for olefin hydrogenation. Indeed, the parallels in the activity of the various actinide complexes for hydrogenation and polymerization, the similarities in maximum percentage of active sites deduced from poisoning experiments, and the observation that H_2 exposure diverts ethylene reactivity from polymerization to hydrogenation are all consistent with both processes occurring at very similar or identical sites. Butene isomerization could also occur in a cycle such as Scheme III, in which olefin addition–elimination sequences (cf., i, ii) would effect double-bond migration. The endothermicity of β-hydride elimination[19] may explain the low activity.

The results of this study provide much information on the stoichiometric and catalytic chemistry of organoactinides on various alumina and silica surfaces. Many of these results are likely generalizable to early transition elements and lanthanides. However, as is frequently the case in catalysts, it is not possible from the available information to generate a completely rigorous structural description of the catalytically active site(s). Still, it is evident that destruction or deactivation of metal–carbon (hydrogen) bond reactivity (e.g., F, G) is detrimental to catalytic activity, while the creation of coordinatively unsaturated, highly electrophilic centers appears desirable. A structure such as or similar to I, which has been identified in the $Cp'_2Th(CH_3)_2$/DA surface NMR studies (vide infra),[7] requires the presence of surface Lewis acid centers (not available for silica[26a,b,d]) and would seem to fulfill many of the latter prerequisites. Future investigations will address these issues under both homogeneous and heterogeneous conditions, as well as explore the scope of surface and catalytic chemistry as a function of f-element complex and support.

Acknowledgment. We are grateful to the Department of Energy for support of this research under Contract DEAC 02-81ER10980. We thank Professor A. M. Seyam, R. S. Sternal, and H. A. Stecher for organoactinide samples. We thank Professor J. B. Butt for helpful discussions.

(41) Otero-Schipper, P. H.; Wachter, W. A.; Butt, J. B.; Burwell, R. L., Jr.; Cohen, J. B. *J. Catal.* **1977**, *50*, 494–507.

(42) (a) Wakefield, B. J. "The Chemistry of Organolithium Compounds"; Pergamon Press: New York, 1974. (b) Becker, W. E.; Ashby, E. C. *J. Org. Chem.* **1964**, *29*, 954–955. (c) Podall, H. E.; Petree, H. E.; Zeitz, J. R. *J. Org. Chem.* **1959**, *24*, 1222–1226. (d) Screttas, C. G.; Eastham, J. F. *J. Am. Chem. Soc.* **1966**, *88*, 5668–5670.

(43) (a) Brintzinger, H. H. *J. Organomet. Chem.* **1979**, *171*, 337–344. (b) Gell, K. I.; Schwartz, J. *J. Am. Chem. Soc.* **1978**, *100*, 3246–3248.

(44) (a) Mauermann, H.; Swepston, P. J.; Marks, T. J. *Organometallics*, in press. (b) Jeske, G.; Lauke, H.; Mauermann, H.; Schumann, H.; Marks, T. J., unpublished results.

(45) (a) Watson, P. L. *J. Am. Chem. Soc.* **1982**, *104*, 337–339. (b) Jeske, G.; Lauke, H.; Mauermann, H.; Swepston, P. N.; Schumann, H.; Marks, T. J., unpublished results.

(46) (a) Sinn, H.; Kaminsky, W. *Adv. Organomet. Chem.* **1980**, *18*, 99–149. (b) Pino, P. *Angew. Chem., Int. Ed. Engl.* **1980**, *19*, 857–875. (c) Yamamoto, A.; Yamamoto, T. *J. Polym. Sci. Macromol. Rev.* **1978**, *13*, 161–218. (d) Chien, J. W., Ed. "Coordination Polymerization"; Academic Press: New York, 1975.